Reliability Engineering and System Safety ▮ (▮▮▮▮) ▮▮▮–▮▮▮

Contents lists available at ScienceDirect

Reliability Engineering and System Safety

journal homepage: www.elsevier.com/locate/ress

Uncertainty and sensitivity analysis in performance assessment for the proposed high-level radioactive waste repository at Yucca Mountain, Nevada

Jon C. Helton [a,*], Clifford W. Hansen [b], Cédric J. Sallaberry [c]

[a] Department of Mathematics and Statistics, Arizona State University, Tempe, AZ 85287-1804, USA
[b] Department 6112, Sandia National Laboratories, Albuquerque, NM 87185-1033, USA
[c] Department 6224, Sandia National Laboratories, Albuquerque, NM 87185-1370, USA

ARTICLE INFO

Article history:
Received 2 November 2010
Received in revised form
23 June 2011
Accepted 6 July 2011

Keywords:
Aleatory uncertainty
Epistemic uncertainty
Performance assessment
Radioactive waste disposal
Sensitivity analysis
Uncertainty analysis
Yucca Mountain

ABSTRACT

Extensive work has been carried out by the U.S. Department of Energy (DOE) in the development of a proposed geologic repository at Yucca Mountain (YM), Nevada, for the disposal of high-level radioactive waste. As part of this development, a detailed performance assessment (PA) for the YM repository was completed in 2008 and supported a license application by the DOE to the U.S. Nuclear Regulatory Commission (NRC) for the construction of the YM repository. The following aspects of the 2008 YM PA are described in this presentation: (i) conceptual structure and computational organization, (ii) uncertainty and sensitivity analysis techniques in use, (iii) uncertainty and sensitivity analysis for physical processes, and (iv) uncertainty and sensitivity analysis for expected dose to the reasonably maximally exposed individual (RMEI) specified the NRC's regulations for the YM repository.

1. Introduction

Extensive work has been carried out by the U.S. Department of Energy (DOE) in the development of a proposed geologic repository at Yucca Mountain (YM), Nevada, for the disposal of high-level radioactive waste [1–6]. As part of this development, a detailed performance assessment (PA) for the YM repository was completed in 2008 [6] and supported a license application by the DOE to the U.S. Nuclear Regulatory Commission (NRC) for the construction of the YM repository [7]. This presentation provides an overview of the conceptual and computational structure of the indicated PA (hereafter referred to as the 2008 YM PA) and the roles that uncertainty analysis and sensitivity analysis play in this structure.

The following aspects of the 2008 YM PA are described in this presentation: (i) conceptual structure and computational organization (Section 2), (ii) uncertainty and sensitivity analysis techniques in use (Section 3), (iii) uncertainty and sensitivity analysis for physical processes (Section 4), and (iv) uncertainty and sensitivity analysis for expected dose to a reasonably maximally exposed individual (RMEI) specified the NRC's regulations for the YM repository (Section 5). The presentation then ends with a summary discussion (Section 6).

This presentation is based on an invited talk given at the 2010 Sensitivity Analysis of Model Output (SAMO) conference in Milan, Italy [8], and, in turn, is an adaptation of three earlier presentations given at the 2008 International High-Level Radioactive Waste Management Conference (IHLRWMC) in Las Vegas, Nevada [9–11]. The primary background reference for this presentation is a large and detailed technical report that describes the 2008 YM PA and provides references to a large body of additional reports that provide further information on the details of the 2008 YM PA and the models incorporated into this PA [6]. Selected aspects of the 2008 YM PA have also been described by the authors of this presentation in three additional conference papers [12–14] and a book chapter [15]. At present, a special issue of *Reliability Engineering & System Safety* is under development that will provide more details on uncertainty and sensitivity analysis in the 2008 YM PA than can be included in a single journal article.

2. Conceptual structure and computational organization

2.1. Regulatory background

The regulatory requirements that underlie the 2008 YM PA derive from the Energy Policy Act of 1992 [16] within which

* Correspondence to: Department 1544, Sandia National Laboratories, Albuquerque, NM 87185-0776, USA. Tel.: +1 505 284 4808; fax: +1 505 284 4002.
E-mail address: jchelto@sandia.gov (J.C. Helton).

0951-8320/$ - see front matter © 2011 Elsevier Ltd. All rights reserved.
doi:10.1016/j.ress.2011.07.002

(i) the U.S. Environmental Protection Agency (EPA) is required to promulgate public health and safety standards for radioactive material stored or disposed of in the YM repository, (ii) the NRC is required to incorporate the EPA standards into licensing standards for the YM repository, and (iii) the DOE is required to show compliance with the NRC standards. The resulting regulatory requirements for the YM repository have two primary sources from the EPA and the NRC, respectively: (i) *Public Health and Environmental Radiation Protection Standards for Yucca Mountain, NV; Final Rule* (40 CFR Part 197) [17] and (ii) *Disposal of High-Level Radioactive Wastes in a Proposed Geologic Repository at Yucca Mountain, Nevada; Final Rule* (10 CFR Parts 2, 19, 20, etc.) [18]. The NRC also published the *Yucca Mountain Review Plan; Final Report* (YMRP) [19] to guide assessing compliance with 10 CFR Parts 2, 19, 20, etc. In turn, the DOE must carry out a PA for the YM repository that satisfies the requirements specified in the preceding documents.

The initial EPA standard [17] specified requirements that the YM repository was to satisfy for the first 10^4 yr after its closure. In a subsequent suit [20], it was ruled that the EPA did not follow guidance in a National Academy of Science (NAS) study [21] as mandated in the Energy Policy Act of 1992. In particular, it was ruled that the EPA had failed to follow guidance that the regulatory period for the YM repository should extend over the period of geologic stability at the repository site, which was suggested to be 10^6 yr. As a result, the initial standard [17] for the YM repository was remanded to the EPA for revision.

In response, the EPA published 40 CFR Part 197, *Public Health and Environmental Radiation Protection Standards for Yucca Mountain, Nevada; Proposed Rule*, which contained proposed revisions to the standards for the YM repository [22]. Consistent with the EPA's proposed revisions, the NRC published 10 CFR Part 63, *Implementation of a Dose Standard After 10,000 Years* [23]. The EPA's and NRC's proposals in response to the remand left most of the requirements for the first 10^4 yr after repository closure unchanged. However, new conditions were proposed for the time interval from 10^4 yr through the period of geologic stability.

The overall structure of the 2008 YM PA derives from the individual protection standard specified by the EPA and the NRC in the revised standards [22,23]. Specifically, the following standard is specified by the NRC ([23], p. 53319):

> § 63.311 Individual protection standard after permanent closure. (a) DOE must demonstrate, using performance assessment, that there is a reasonable expectation that the reasonably maximally exposed individual receives no more than the following annual dose from releases from the undisturbed Yucca Mountain disposal system: (1) 0.15 mSv (15 mrem) for 10,000 years following disposal; and (2) 3.5 mSv (350 mrem) after 10,000 years, but within the period of geologic stability. (b) DOE's performance assessment must include all potential environmental pathways of radionuclide transport and exposure. (NRC1).

Except for minor differences in wording, the preceding standard is the same as the proposed standard specified by the EPA ([22], p. 49063).

In turn, the NRC gives the following guidance on implementing the preceding individual protection standard ([23], p. 53319):

> § 63.303 Implementation of Subpart L. (a) Compliance is based upon the arithmetic mean of the projected doses from DOE's performance assessments for the period within 10,000 years after disposal for: (1) § 63.311(a)(1); and (2) §§ 63.321(b)(1) and 63.331, if performance assessment is used to demonstrate compliance with either or both of these sections. (b) Compliance is based upon the median of the projected doses from DOE's performance assessments for the period after 10,000 years of disposal and through the period of geologic stability for: (1) § 63.311(a)(2); and (2) § 63.321(b)(2), if performance assessment is used to demonstrate compliance. (NRC2)

Again, the preceding is the same as the corresponding guidance given by the EPA ([22], p. 49063).

As indicated in (NRC1) and (NRC2), the NRC expects the determination of mean and median dose to the reasonably maximally exposed individual (RMEI) to be based on a detailed PA. This expectation is further emphasized by the following statement in the YMRP ([19], p. 2.2-1):

> Risk-Informed Review Process for Performance Assessment—The performance assessment quantifies repository performance, as a means of demonstrating compliance with the postclosure performance objectives at 10 CFR 63.113. The U.S. Department of Energy performance assessment is a systematic analysis that answers the triplet risk questions: what can happen; how likely is it to happen; and what are the consequences. (NRC3)

For convenience, the preceding questions can be represented by Q1, "What can happen?", Q2, "How likely is it to happen?", and Q3, "What are the consequences if it does happen?". The preceding questions provide the intuitive basis for the Kaplan/Garrick ordered triple representation for risk:

$$(\mathcal{S}_i, pS_i, \mathbf{cS}_i), \quad i = 1,2,\ldots,nS, \tag{1}$$

where (i) $\mathcal{S}_i$ is a set of similar occurrences (i.e., the answer to Q1), (ii) pS_i is the probability of $\mathcal{S}_i$ (i.e., the answer to Q2), and (iii) $\mathbf{cS}_i$ is a vector of consequences associated with $\mathcal{S}_i$ (i.e., the answer to Q3) [24]. Further, the $\mathcal{S}_i$ must be disjoint (i.e., $\mathcal{S}_i \cap \mathcal{S}_j = \emptyset$ for $i \neq j$); each $\mathcal{S}_i$ must be sufficiently homogeneous to allow use of a single representative consequence vector $\mathbf{cS}_i$; and $\cup_i \mathcal{S}_i$ must contain all risk significant occurrences for the facility under consideration.

In addition, there is a fourth basic question that underlies the 2008 YM PA and, indeed, all complete PAs: Q4, "What is the uncertainty in the answers to the initial three questions?". The importance of answering this fourth question is emphasized in a number of statements by the NRC. For example:

> For such long-term performance, what is required is reasonable expectation, making allowance for the time period, hazards, and uncertainties involved, that the outcome will conform with the objectives for postclosure performance for the geologic repository. Demonstrating compliance will involve the use of complex predictive models that are supported by limited data from field and laboratory tests, site-specific monitoring, and natural analog studies that may be supplemented with prevalent expert judgment. Compliance demonstrations should not exclude important parameters from assessments and analyses simply because they are difficult to precisely quantify to a high degree of confidence. The performance assessments and analyses should focus upon the full range of defensible and reasonable parameter distributions rather than only upon extreme physical situations and parameter values ([18], p. 55804). (NRC4)

> Once again, although the criteria may be written in unqualified terms, the demonstration of compliance must take uncertainties and gaps in knowledge into account so that the Commission can make the specified finding with respect to paragraph (a)(2) of § 63.31 ([18], p. 55804). (NRC5)

Both the preceding statements clearly indicate that a reasonable treatment of uncertainty should be a fundamental part of a PA used to support a licensing application for the YM repository.

Please cite this article as: Helton JC, et al. Uncertainty and sensitivity analysis in performance assessment for the proposed high-level radioactive waste repository at Yucca Mountain, Nevada. Reliab Eng Syst Safety (2011), doi:10.1016/j.ress.2011.07.002

When the design and implementation of the analysis that would become the 2008 YM PA began in the 2005–2006 time frame, the regulatory requirements in Refs. [22,23] as indicated in Quotes (NRC1)–(NRC5) provided the primary design guidance. However, during and subsequent to the 2006–2007 time frame, the appropriateness of the post 10^4 yr requirements was under active consideration. In particular, the appropriateness of the 350 mrem/yr requirement for dose to the RMEI and also the appropriateness of basing the dose requirement on a median dose rather than on a mean (i.e., expected) dose were under consideration. As a consequence, a change in the post 10^4 yr dose requirement from a bound on a median dose to a bound on a mean dose in the final regulations for the YM repository was a real possibility that had to planned for. Because of this uncertainty, the 2008 YM PA was designed to calculate both median and mean doses as indicated in Sections 2.2–2.4 and illustrated in Sections 4 and 5.

As it turned out, changes were indeed made to the post 10^4 yr dose requirements for the YM repository: (i) the 350 mrem/yr requirement for dose to the RMEI was reduced to 100 mrem/yr, and (ii) the use of a mean (i.e., expected) dose was specified instead of a median dose. Specifically, the NRC promulgated the following revised requirements [25, p. 10829]:

> § 63.311 Individual protection standard after permanent closure. (a) DOE must demonstrate, using performance assessment, that there is a reasonable expectation that the reasonably maximally exposed individual receives no more than the following annual dose from releases from the undisturbed Yucca Mountain disposal system: (1) 0.15 mSv (15 mrem) for 10,000 years following disposal; and (2) 1.0 mSv (100 mrem) after 10,000 years, but within the period of geologic stability. (b) DOE's performance assessment must include all potential environmental pathways of radionuclide transport and exposure. (NRC6)

> § 63.303 Implementation of Subpart L. (a) Compliance is based upon the arithmetic mean of the projected doses from DOE's performance assessments for the period within 1 million years after disposal, with: (1) Sections 63.311(a)(1) and 63.311(a)(2); and (2) Sections 63.321(b)(1), 63.321(b)(2) and 63.331, if performance assessment is used to demonstrate compliance with either or both of these sections. (NRC7)

The preceding is the same as the corresponding guidance given by the EPA ([26], pp. 6187–882) and constitutes the core dose requirements that the YM repository must satisfy.

Additional discussion of the regulatory requirements that underlie the 2008 YM PA is available in Refs. [27,28] and App. J of Ref. [6].

2.2. Conceptual structure

The 2008 YM PA was developed to satisfy requirements in 10 CFR Part 63 [25] and has a structure that involves three basic entities: EN1, a characterization of the uncertainty in the occurrence of future events (e.g., igneous events, seismic events) that could affect the performance of the repository; EN2, models for predicting the physical behavior and evolution of the repository (e.g., systems of ordinary and partial differential equations); and EN3, a characterization of the uncertainty associated with analysis inputs that have fixed but imprecisely known values (e.g., the spatially averaged value for a distribution coefficient) [29,30]. The designators aleatory and epistemic are commonly used for the uncertainties characterized by EN1 and EN3, respectively [24,31–40].

In the preceding, aleatory uncertainty is used in the designation of randomness in the possible future conditions that could affect the YM repository. In concept, each possible future at the YM repository can be represented by a vector

$$\mathbf{a} = [a_1, a_2, \ldots, a_{nA}], \tag{2}$$

where each a_i is a specific property of the future $\mathbf{a}$ (e.g., time of a seismic event, size of a seismic event, …). In turn, a subset $\mathcal{S}$ of the set $\mathcal{A}$ of all possible values for $\mathbf{a}$ constitutes what is referred to as a scenario class in the 2008 YM PA. As part of the 2008 YM PA development, a probabilistic structure is imposed on the set $\mathcal{A}$. Formally, this corresponds to defining a probability space ($\mathcal{A}$, $\mathbb{A}$, p_A) for aleatory uncertainty ([41], Section 4.3). Then, $\mathbb{A}$ is the set of all possible scenario classes, and p_A is the function that defines scenario class probability (i.e., scenario class $\mathcal{S}$ is an element of $\mathbb{A}$ and $p_A(\mathcal{S})$ is the probability of scenario class $\mathcal{S}$). As discussed in more detail in Section 2.5, the set $\mathbb{A}$ contains both disjoint and nondisjoint scenario classes. Formally, the probability space ($\mathcal{A}$, $\mathbb{A}$, p_A) provides a characterization of aleatory uncertainty and constitutes the first of the three basic mathematical entities that underlie the determination of expected (i.e., mean) dose.

Although useful conceptually and notationally, the probability space ($\mathcal{A}$, $\mathbb{A}$, p_A) is never explicitly defined in the 2008 YM PA. Rather, the characterization of aleatory uncertainty enters the analysis through the definition of probability distributions for the individual elements of $\mathbf{a}$. Conceptually, the distributions for the elements of $\mathbf{a}$ lead to a distribution for $\mathbf{a}$ and an associated density function $d_A(\mathbf{a})$. The nature of the probability space ($\mathcal{A}$, $\mathbb{A}$, p_A) in the context of the 2008 YM PA is summarized in Table 1 (see [6], App. J, for additional information).

The second of the three basic mathematical entities that underlie the determination of expected dose is a model that estimates dose to the RMEI. Formally, this model can be represented by

Table 1
Representation of aleatory uncertainty in the 2008 YM PA [9], Table I and [15] Table 17.1; see [6], Section J4.4 for additional discussion.

Individual futures:

$\mathbf{a} = [nEW, nED, nII, nIE, nSG, nSF, \mathbf{a}_{EW}, \mathbf{a}_{ED}, \mathbf{a}_{II}, \mathbf{a}_{IE}, \mathbf{a}_{SG}, \mathbf{a}_{SF}]$

where, for a time interval $[a, b]$ (e.g., $[0, 10^4$ yr] or $[0, 10^6$ yr]), nEW = number of early waste package (WP) failures, nED = number of early drip shield (DS) failures, nII = number of igneous intrusive (II) events, nIE = number of igneous eruptive (IE) events, nSG = number of seismic ground (SG) motion events, nSF = number of seismic fault (SF) displacement events, $\mathbf{a}_{EW}$ = vector defining the nEW early WP failures, $\mathbf{a}_{ED}$ = vector defining the nED early DS failures, $\mathbf{a}_{II}$ = vector defining the nII igneous intrusive events, $\mathbf{a}_{IE}$ = vector defining the nIE igneous eruptive events, $\mathbf{a}_{SG}$ = vector defining the nSG seismic ground motion events, and $\mathbf{a}_{SF}$ = vector defining the nSF seismic fault displacement events.

Sample space for aleatory uncertainty:

$\mathcal{A} = \{\mathbf{a} : \mathbf{a} = [nEW, nED, nII, nIE, nSG, nSF, \mathbf{a}_{EW}, \mathbf{a}_{ED}, \mathbf{a}_{II}, \mathbf{a}_{IE}, \mathbf{a}_{SG}, \mathbf{a}_{SF}]\}$

Example scenario classes:

Nominal, $\mathcal{A}_N = \{\mathbf{a} : \mathbf{a} \in \mathcal{A} \text{ and } nEW = nED = nII = nIE = nSG = nSF = 0\}$
Early WP failure, $\mathcal{A}_{EW} = \{\mathbf{a} : \mathbf{a} \in \mathcal{A} \text{ and } nEW \geq 1\}$
Early DS failure, $\mathcal{A}_{ED} = \{\mathbf{a} : \mathbf{a} \in \mathcal{A} \text{ and } nED \geq 1\}$
Igneous intrusive, $\mathcal{A}_{II} = \{\mathbf{a} : \mathbf{a} \in \mathcal{A} \text{ and } nII \geq 1\}$
Igneous eruptive, $\mathcal{A}_{IE} = \{\mathbf{a} : \mathbf{a} \in \mathcal{A} \text{ and } nIE \geq 1\}$
Seismic ground motion, $\mathcal{A}_{SG} = \{\mathbf{a} : \mathbf{a} \in \mathcal{A} \text{ and } nSG \geq 1\}$
Seismic fault displacement, $\mathcal{A}_{SF} = \{\mathbf{a} : \mathbf{a} \in \mathcal{A} \text{ and } nSF \geq 1\}$
Early failure, $\mathcal{A}_E = \mathcal{A}_{EW} \cup \mathcal{A}_{ED}$, Igneous, $\mathcal{A}_I = \mathcal{A}_{II} \cup \mathcal{A}_{IE}$, Seismic, $\mathcal{A}_S = \mathcal{A}_{SG} \cup \mathcal{A}_{SF}$

Scenario class probabilities:

$p_A(\mathcal{A}_N)$ = probability of no disruptions of any kind; $p_A(\mathcal{A}_{EW})$ = probability of one or more early WP failures; $p_A(\mathcal{A}_{ED})$ = probability of one or more early DS failures; $p_A(\mathcal{A}_{II})$ = probability of one or more II events; $p_A(\mathcal{A}_{IE})$ = probability of one or more IE events; $p_A(\mathcal{A}_{SG})$ = probability of one or more SG motion events; $p_A(\mathcal{A}_{SF})$ = probability of one or more SF displacement events; $p_A(\mathcal{A}_E)$ = probability of one or more early failures; $p_A(\mathcal{A}_I)$ = probability of one or more igneous events; $p_A(\mathcal{A}_S)$ = probability of one or more seismic events

Please cite this article as: Helton JC, et al. Uncertainty and sensitivity analysis in performance assessment for the proposed high-level radioactive waste repository at Yucca Mountain, Nevada. Reliab Eng Syst Safety (2011), doi:10.1016/j.ress.2011.07.002

the function

$$D(\tau|\mathbf{a}) = \text{dose to RMEI (mrem/yr) at time } \tau \text{ (yr) conditional on the occurrence of the future represented by } \mathbf{a}. \quad (3)$$

Technically, $D(\tau|\mathbf{a})$ is the committed 50 yr dose to the RMEI that results from radiation exposure incurred in a single year. In the computational implementation of the 2008 YM PA, $D(\tau|\mathbf{a})$ is only one of the results calculated for the particular analysis configuration defined for the future $\mathbf{a}$. In practice, many results are calculated for $\mathbf{a}$ in addition to dose to the RMEI (see examples in Section 4 and a complete listing in Table K3-4 of Ref. [6]). Thus, $D(\tau|\mathbf{a})$ is actually part of a vector containing a large number of elements. The general nature of the models that constitute $D(\tau|\mathbf{a})$ is described in several conference presentations [42–44] and in more detail in Ref. [6]. As an example, an overview of the structure of the models that correspond to $D(\tau|\mathbf{a})$ for seismic conditions in the 2008 YM PA is presented in Fig. 1.

The third of the three basic mathematical entities that underlie the determination of expected dose is a probabilistic characterization of epistemic uncertainty. Here, epistemic uncertainty refers to a lack of knowledge with respect to the appropriate value to use for a quantity that is assumed to have a constant or fixed value in the context of a particular analysis. Specifically, epistemic uncertainty relates to a vector of the form

$$\begin{aligned}\mathbf{e} &= [\mathbf{e}_A, \mathbf{e}_M] \\ &= [e_{A1}, e_{A2}, \ldots, e_{A,nAE}, e_{M1}, e_{M2}, \ldots, e_{M,nME}] \\ &= [e_1, e_2, \ldots, e_{nE}], \quad nE = nAE + nME, \end{aligned} \quad (4)$$

where

$$\mathbf{e}_A = [e_{A1}, e_{A2}, \ldots, e_{A,nAE}]$$

is a vector of epistemically uncertain quantities used in the characterization of aleatory uncertainty (e.g., a rate term that defines a Poisson process) and

$$\mathbf{e}_M = [e_{M1}, e_{M2}, \ldots, e_{M,nME}]$$

is a vector of epistemically uncertain quantities used in the determination of dose (e.g., a distribution coefficient).

Epistemic uncertainty results in a set $\mathcal{E}$ of possible values for $\mathbf{e}$. In turn, probability is used to characterize the level of likelihood or credence that can be assigned to various subsets of $\mathcal{E}$. In concept, this leads to a probability space $(\mathcal{E}, \mathbb{E}, p_E)$ for epistemic uncertainty. Like the probability space $(\mathcal{A}, \mathbb{A}, p_A)$ for aleatory uncertainty, the probability space $(\mathcal{E}, \mathbb{E}, p_E)$ for epistemic uncertainty is useful conceptually and notationally but is never explicitly defined in the 2008 YM PA. Rather, the characterization of epistemic uncertainty enters the analysis through the definition of probability distributions for the individual elements of $\mathbf{e}$. These distributions serve as mathematical summaries of all available information with respect to where the appropriate values for individual elements of $\mathbf{e}$ are located for use in the 2008 YM PA. Conceptually, the distributions for the elements of $\mathbf{e}$ lead to a distribution for $\mathbf{e}$ and an associated density function $d_E(\mathbf{e})$. The nature of the probability space $(\mathcal{E}, \mathbb{E}, p_E)$ in the context of the 2008 YM PA is indicated in Table 2 (see [6], Tables K3-1, K3-2, K3-3, and Refs. [6,45–57] cited in Table 2 for additional information). The variables listed in Table 2 were selected on the basis of their identification in the sensitivity analyses presented in Sections 4 and 5.

2.3. Expected dose, mean dose, median dose

Now that the characterization of epistemic uncertainty has been introduced, the notations used to represent aleatory uncertainty and dose need to be expanded. Because the representation of aleatory uncertainty depends on elements of the vector $\mathbf{e}_A$, each possible value for $\mathbf{e}_A$ could lead to a different probability space $(\mathcal{A}, \mathbb{A}, p_A)$ for aleatory uncertainty. For notational convenience, this dependence will be indicated by representing the density function associated with aleatory uncertainty by $d_A(\mathbf{a}|\mathbf{e}_A)$. Similarly, the determination of dose depends on elements of the vector $\mathbf{e}_M$, with each possible value for $\mathbf{e}_M$ potentially leading to different dose results. For notational convenience, this dependence will be indicated by representing the dose function by $D(\tau|\mathbf{a},\mathbf{e}_M)$.

The probability space $(\mathcal{A}, \mathbb{A}, p_A)$ for aleatory uncertainty characterized by the density function $d_A(\mathbf{a}|\mathbf{e}_A)$, the dose function $D(\tau|\mathbf{a},\mathbf{e}_M)$, and the probability space $(\mathcal{E}, \mathbb{E}, p_E)$ for epistemic uncertainty characterized by the density function $d_E(\mathbf{e})$ constitute the three basic components of the 2008 YM PA that come together in the determination of expected dose to the RMEI and the uncertainty in expected dose to the RMEI. Specifically, the expected value for dose at time τ conditional on a specific element $\mathbf{e} = [\mathbf{e}_A, \mathbf{e}_M]$ of $\mathcal{E}$ is defined by

$$\overline{D}(\tau|\mathbf{e}) = E_A[D(\tau|\mathbf{a},\mathbf{e}_M)|\mathbf{e}_A] = \int_{\mathcal{A}} D(\tau|\mathbf{a},\mathbf{e}_M) d_A(\mathbf{a}|\mathbf{e}_A) \mathrm{d}A, \quad (5)$$

where $E_A[D(\tau|\mathbf{a},\mathbf{e}_M)|\mathbf{e}_A]$ denotes expectation over aleatory uncertainty.

In turn, the uncertainty associated with the estimation of $\overline{D}(\tau|\mathbf{e})$ can be determined from the properties of the probability space $(\mathcal{E}, \mathbb{E}, p_E)$ for epistemic uncertainty. In particular, the cumulative distribution function (CDF) for $\overline{D}(\tau|\mathbf{e})$ and the expected value for $\overline{D}(\tau|\mathbf{e})$ that derive from epistemic uncertainty are given by

$$\begin{aligned} p_E[\overline{D}(\tau|\mathbf{e}) \le D] &= \int_{\mathcal{E}} \underline{\delta}_D[\overline{D}(\tau|\mathbf{e})] d_E(\mathbf{e}) \mathrm{d}E \\ &= \int_{\mathcal{E}} \underline{\delta}_D \left[\int_{\mathcal{A}} D(\tau|\mathbf{a},\mathbf{e}_M) d_A(\mathbf{a}|\mathbf{e}_A) \mathrm{d}A \right] d_E(\mathbf{e}) \mathrm{d}E \end{aligned} \quad (6)$$

and

$$\overline{\overline{D}}(\tau) = E_E[\overline{D}(\tau|\mathbf{e})] = \int_{\mathcal{E}} \overline{D}(\tau|\mathbf{e}) d_E(\mathbf{e}) \mathrm{d}E, \quad (7)$$

respectively, where

$$\underline{\delta}_D[\overline{D}(\tau|\mathbf{e})] = \begin{cases} 1 & \text{if } \overline{D}(\tau|\mathbf{e}) \le D \\ 0 & \text{if } \overline{D}(\tau|\mathbf{e}) > D \end{cases}$$

and $E_E[\overline{D}(\tau|\mathbf{e})]$ denotes expectation over epistemic uncertainty.

The individual gray curves in Fig. 2 correspond to expected doses $\overline{D}(\tau|\mathbf{e})$ as defined in Eq. (5). The totality of the gray curves provides a display of the uncertainty in $\overline{D}(\tau|\mathbf{e})$ that derives from the uncertainty in $\mathbf{e}$. The solid curve in Fig. 2 corresponds to the mean dose $\overline{\overline{D}}(\tau)$ defined in Eq. (7) and used in comparisons with the 10^4 yr standard as specified in Quotes (NRC1) and (NRC2). Specifically, $\overline{\overline{D}}(\tau)$ is the expected value for $\overline{D}(\tau|\mathbf{e})$ over the epistemic uncertainty associated with $\mathbf{e}$.

The value of D for which

$$q = p_E[\overline{D}(\tau|\mathbf{e}) \le D] = \int_{\mathcal{E}} \underline{\delta}_D[\overline{D}(\tau|\mathbf{e})] d_E(\mathbf{e}) \mathrm{d}E \quad (8)$$

defines the q quantile (e.g., $q = 0.05, 0.5, 0.95$) for the distribution of expected dose over epistemically uncertain analysis inputs at time τ. For notational purposes, the value of D corresponding to the q quantile of $\overline{D}(\tau|\mathbf{e})$ defined in Eq. (8) will be represented by $Q_{E,q}[\overline{D}(\tau|\mathbf{e})]$. The median curve in Fig. 2 corresponds to the median dose $Q_{E,0.5}[\overline{D}(\tau|\mathbf{e})]$ defined in Eq. (8) for $q = 0.5$. Prior to the change in the post 10^4 yr requirements from a bound on a median dose as indicated in (NRC1) and (NRC2) to a bound on a mean dose as indicated in (NRC6) and (NRC7), $Q_{E,0.5}[\overline{D}(\tau|\mathbf{e})]$ was the quantity specified for use in comparisons with the post 10^4 yr requirements. After the change indicated in (NRC6) and (NRC7), the mean dose $\overline{\overline{D}}(\tau)$ defined in Eq. (7) is used in comparisons with both the pre and post 10^4 yr requirements.

Please cite this article as: Helton JC, et al. Uncertainty and sensitivity analysis in performance assessment for the proposed high-level radioactive waste repository at Yucca Mountain, Nevada. Reliab Eng Syst Safety (2011), doi:10.1016/j.ress.2011.07.002

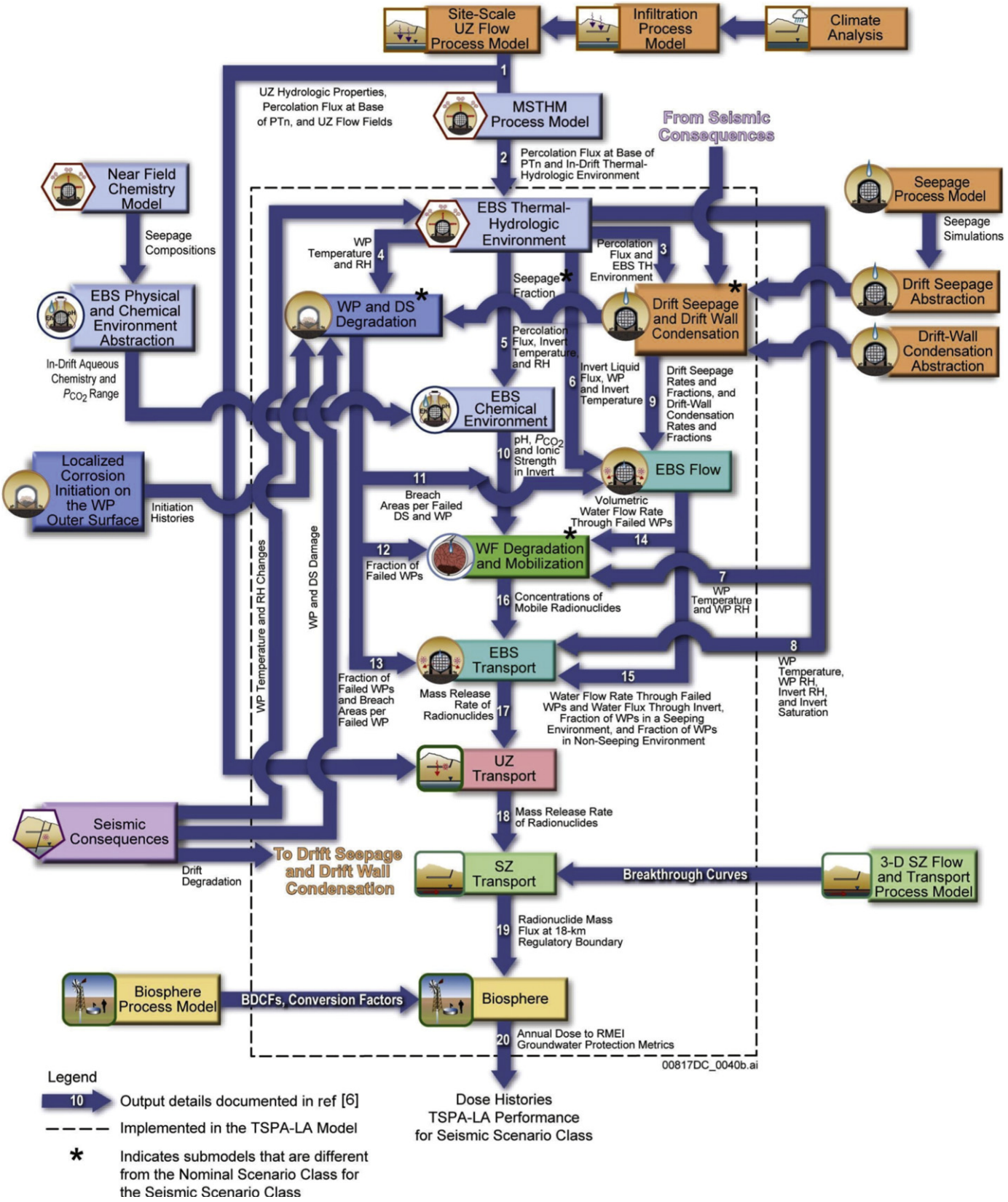

Fig. 1. Information transfer between the model components and submodels for the seismic scenario class in the 2008 YM PA ([6], Fig. 6.1.4-6).

2.4. Computational implementation

Evaluation of expected, mean and median doses as described in the preceding section presents two numerical challenges. First, it is necessary to evaluate integrals over the set $\mathcal{A}$ to obtain expected doses over aleatory uncertainty. Second, it is necessary to evaluate integrals over the set $\mathcal{E}$ to obtain mean and median doses over aleatory and epistemic uncertainty.

Please cite this article as: Helton JC, et al. Uncertainty and sensitivity analysis in performance assessment for the proposed high-level radioactive waste repository at Yucca Mountain, Nevada. Reliab Eng Syst Safety (2011), doi:10.1016/j.ress.2011.07.002

Table 2
Examples of the $nE=392$ epistemically uncertain variables considered in the 2008 YM PA (see [6], Tables K3-1, K3-2, K3-3, for a complete listing of the epistemically uncertain variables considered in the 2008 YM PA).

DASHAVG. Mass median ash particle diameter (cm). *Distribution:* Log triangular. *Range:* 0.001–0.1. *Mode:* 0.01. *Additional information:* [6 (Table 6.5-4), 45 (Sections 6.5.2.4, 7.2, 7.7, App. C, Tables 4-1, 6-3, 8-2 and C-3, and Fig. C-2)]
DDIVIDE. Diffusivity of radionuclides in divides of the Fortymile Wash fan (RMEI location) (cm^2/yr). *Distribution:* uniform. *Range:* 0.001–0.095. *Mean* 0.048. *Additional information:* [6 (Table 6.5-5), 45 (Sections 6.5.8.1, 6.6.2 and 7.1.3, and Tables 6.4-1, 6.5.8-1 and 6.6.2-1)]
DELPPCO2. Selector variable for partial pressure of CO_2 (dimensionless). *Distribution:* uniform. *Range:* -1 to 1. *Additional information:* [6 (Sections 6.3.4.2 and 6.3.5.2.3, and Table 6.3.5-4), 46 (Sections 6.1, 67.2, 6.9.1, 6.12.2.1, 6.12.4.2, 6.13, 6.15.1, 7.1.2.2, 7.1.3.3, 7.1.4.2 and 7.2.3)]
DSNFMASS. Scale factor used to characterize uncertainty in radionuclide content of defense spent nuclear fuel (DSNF) (dimensionless). *Distribution:* triangular. *Range:* 0.45–2.9. *Mode:* 0.62. *Additional information:* [6 (Sections 6.3.7.1.2 and 6.3.7.1.3 and Table 6.3.7-7), 47 (Sections 6.6.2, 6.7 and 7 and Table 7-2)]
EP1LOWAM. Logarithm of the scale factor used to characterize uncertainty in americium solubility at an ionic strength below 1 molal (dimensionless) *Distribution:* Truncated normal. *Range:* -2 to 2. *Mean:* 0. *Standard deviation:* 1. *Additional information:* [6 (Sections 6.3.7.5.1, 6.3.7.5.2 and 6.3.7.5.3, Table 6.3.7-41, and Eq. 6.3.7-13a), 48 (Sections 6.9 and 8.1.2, Eqs. 6.9-1 and 8.1, and Table 6.9-4)]
EP1LOWPU. Logarithm of the scale factor used to characterize uncertainty in plutonium solubility at an ionic strength below 1 molal (dimensionless). *Distribution:* Truncated normal. *Range:* -1.4 to 1.4. *Mean:* 0. *Standard deviation:* 0.7. *Additional information:* [6 (Sections 6.3.7.5.1, 6.3.7.5.2 and 6.3.7.5.3, Table 6.3.7-44, and Eq. 6.3.7-13a), 48 (Sections 6.5 and 8.1.2, Eqs. 6.5-1, 6.5-2 and 8-1, and Table 6.5-5)]
EP1NPO2. Logarithm of the scale factor used to characterize uncertainty in NpO_2 solubility at an ionic strength below 1 molal (dimensionless). *Distribution:* Truncated normal. *Range:* -1.2 to 1.2. *Mean:* 0. *Standard deviation:* 0.6. *Additional information:* [6 (Sections 6.3.7.5.1, 6.3.7.5.2 and 6.3.7.5.3, Table 6.3.7-43, and Eq. 6.3.7-13a), 48 (Sections 6.6 and 8.1.2, Eqs. 6.6-2 and 8-1, and Table 6.6v5)]
IGERATE. Frequency of occurrence of volcanic eruptive events (yr^{-1}). *Calculated by: IGRATE* $\times$ 0.083. *Range:* 0–6.44E$-$08. *Additional information:* [6 (Section 6.5.2.1.1, App. J, and Eq. J7.5-3), 49 (Table 6-5 and Fig. 7-2)]
IGRATE. Frequency of intersection of the repository footprint by a volcanic event (yr^{-1}). *Distribution:* piecewise uniform. *Range:* 0–7.76E$-$07. *Additional information:* [6 (Table 6.5-2), 50 (Sections 6.1, 6.1.1, 6.3, 6.3.1.5, 6.3.1.8, 6.4.2, 6.5, 6.5.1.1, 6.5.2.1, App. A, Figs. 6–8, 6-23 and 6-24, and Tables 6-5 and 7-1)]
INFIL. Pointer variable for determining infiltration conditions: 10th, 30th, 50th or 90th percentile infiltration scenario (dimensionless). *Distribution:* discrete. *Range:* 1–4. *Additional information:* [6], Section 6.3.1.2, and Tables 6.3.1-2 and 6.3.5-4
INHLTPV. Pointer variable for long-term inhalation dose conversion factor for volcanic ash exposure (dimensionless). *Distribution:* discrete. *Range:* 1–300. *Additional information:* [6 (Section 6.3.11 and Eq. 6.3.11-4), 51 (Sections 6.12.2 and 6.14.5, Table 6.12-2, and Fig. 6.14-2)]
MICC14. Groundwater biosphere dose conversion factor (BDCF) for ^{14}C in modern interglacial climate ($(Sv/yr)/(Bq/m^3)$). *Distribution:* discrete. *Range:* 7.18E$-$10 to 2.56E$-$08. *Mean:* 1.93E$-$09. *Standard Deviation:* 1.85E$-$09. *Additional information:* [6 (Sections 6.3.11.2 and 6.3.11.3 and Table 6.3.11-3), 51 (Sections 1, 6.1, 6.4, 6.4.10, 6.8.10, 6.11 and 6.13, Eqs. 6.4.10-2, 6.4.10-4, 6.2.10-5 and 6.11-5, and Tables 6.11-8 and 6.11-12)]
MICTC99. Groundwater biosphere dose conversion factor (BDCF) for ^{99}Tc in modern interglacial climate ($(Sv/yr)/(Bq/m^3)$). *Distribution:* discrete. *Range:* 5.28E$-$10 to 2.85E$-$08. *Mean:* 1.12E$-$09. *Standard deviation:* 1.26E$-$09. *Additional information:* Same as *MICC14*
PHCSS. Pointer variable used to determine pH in commercial spent nuclear fuel (CSNF) Cell 1 under liquid influx conditions (dimensionless). *Distribution:* Uniform. *Range:* 0–1. *Additional information:* [6], Section 6.3.7.2.2 Part IV.
PROBDSEF. Probability for undetected defects in a drip shield (dimensionless). *Distribution:* Log-normal. *Median:* 4.3E$-$07. *Error factor:* 14. *Additional information:* [6 (Section 6.4.1 and Tables 6.4-1 and 6.4-2), 52 (Sections 6.4, 6.5 and 7.1, Tables 6-10 and 7-1, and Fig. 6-21)]
PROBWPEF. Probability for undetected defects in a waste package (dimensionless). *Distribution:* Log-normal. *Median:* 4.14E$-$05. *Error factor:* 8.17. *Additional information:* [6 (Section 6.4.2 and Tables 6.4-1 and 6.4-2), 52 (Sections 6.3, 6.5 and 7.1, Tables 6-9 and 7-1, and Fig. 6-20)]
SCCTHR. Residual stress threshold for stress corrosion cracking (MPa). *Distribution:* Uniform. *Range:* 315.9 to 368.55. *Additional Information:* [6 (Table 6.3.5-3), 53 (Sections 6.1.1, 6.2.2 and 8.1.1 and Tables 6-3, 8-3 and 8-15)]
SCCTHRP. Residual stress threshold for SCC nucleation of Alloy 22 (as a percentage of yield strength in MPa) (dimensionless); see *SCCTHR* . *Distribution:* uniform. *Range:* 90–105. *Additional information:* [6 (Section 6.6.1.3.7 and Table 6.6-2), 53 (Sections 6.1.1, 6.2.2 and 8.1.1 and Tables 6-3, 8-3 and 8-15)]
SEEPPRM. Logarithm of the mean fracture permeability in lithophysal rock units (dimensionless). *Distribution:* Triangular. *Range:* -0.92 to 0.92. *Mode:* 0. *Additional information:* [6 (Sections 6.3.5.2.3, 6.3.3.1.2 and 6.3.3.1.3 and Tables 6.3.5-4, 6.3.3-2 and 6.3.3-3), 54 (Section 6.6.3)]
SEEPUNC. Uncertainty factor to account for small-scale heterogeneity in fracture permeability (dimensionless). *Distribution:* Uniform. *Range:* 0–1. *Additional information:* [6 (Section 6.3.3.1.2 and Tables 6.3.3-3 and 6.3.5-4), 54 (Sections 6.5.1.3, 6.5.2.2, 6.8 and 8.1 and Tables 6.8-3 and 6-12[a])]
SZCOLRAL. Logarithm of colloid retardation factor in alluvium (dimensionless). *Distribution:* Piecewise uniform. *Range:* 0.903–3.715. *Additional information:* [6 (Sections 6.3.10.1, 6.3.10.2 and 6.3.10.4.2 and Table 6.3.10-2), 55 (Sections 6.3.1, 6.5.1.1 and 6.5.2.11, Tables 4-3, 6-8, A-1[a] and B-1, Eqs. 6-2 and 6-10, and Fig. 6-22)]
SZFIPOVO. Logarithm of flowing interval porosity in volcanic units (dimensionless). *Distribution:* piecewise uniform. *Range:* -5 to -1 *mean/median/mode:* -3. *Additional information:* [6 (Table 6.3.10-2), 55 (Sections 6.5.1.1, 6.5.1.2, 6.5.2.5, 6.5.2.15, B-2[a], 7-1[b] and A-1[b] and Tables 6-8, 7-1[a], A-1[a] and B-1)]
SZGWSPDM. Logarithm of the scale factor used to characterize uncertainty in groundwater specific discharge (dimensionless). *Distribution:* piecewise uniform. *Range:* -0.951 to 0.951. *Additional information:* [6 (Section 6.3.10.2 and Table 6.3.10-2), 55 (Sections 6.5.1.2[a], 6.5.2.1[a], 6.5.3[a] and 8.1[a], Table 6-7[a], 7-1[a] and A-1[a], and Fig. 6-2[a])]
THERMCON. Selector variable for one of three host-rock thermal conductivity scenarios (low, mean, and high) (dimensionless). *Distribution:* discrete. *Range:* 1–3. *Additional information:* [6 (Sections 6.3.2.2, 6.3.2.3, 6.3.5.1.3, 6.3.5.2.3 and 6.6.2.2 and Tables 6.3.2-1, 6.3.2-3 and 6.3.5-4), 56 (Sections 6.2.13.3[a], 6.3.4[a] and 6.3.16[a] and Tables 6.3-47[a] and 6.3-48[a])]
WDGCA22. Temperature dependent slope term of Alloy 22 general corrosion rate (K). *Distribution:* truncated normal. *Range:* 666–7731. *Mean:* 4905. *Standard deviation:* 1413. *Additional information:* [6 (Sections 6.3.5.1.2 and 6.3.5.1.3, Tables 6.3.5-3 and 6.3.5-4, and Eq. 6.3.5-4), 57 (Sections 6.4.3 and 6.4.3.4)]
WDGCUA22. Variable for selecting distribution for general corrosion rate (low, medium, or high) (dimensionless). *Distribution:* discrete. *Range:* 1–3. *Additional information:* [6 (Table 6.3.5-4), 57 (Sections 6.4.3 and 6.4.3.3, Table 6-7, and Fig. 6-23)]
WDNSCC. Stress corrosion cracking growth rate exponent (repassivation slope) (dimensionless). *Distribution:* truncated normal. *Range:* 0.935–1.395. *Mean:* 1.165. *Standard deviation:* 0.115. *Additional information:* [6 (Sections 6.3.5.1.2 and 6.3.5.4, Table 6.3.5-3, and Eqs. 6.3.5-13 and 6.3.5-14), 53 (Sections 6.4.4.4, 8.4.2.3 and 8.4.3, Tables 6-7, 8-1, 8-5, 8-6 and 8-15, and Eqs. 4, 5, 70 and 71)]
WDZOLID. Deviation from median yield strength range for outer lid (dimensionless). *Distribution:* truncated normal. *Range:* -3 to 3. *Mean:* 0. *Standard deviation:* 1. *Additional information:* [6, Sections 6.3.5.1.2 and 6.3.5.1.3 and Table 6.3.5-3, 53 (Sections 6.5.6.5 and 8.4.2.2, Table 8-15, and Eq. 67)]

Evaluation of integrals over the set $\mathcal{A}$ is considered first. These evaluations are accomplished under the assumption that there are no synergisms between the effects of the disruptions associated with the individual scenario classes that have a significant effect on the expected dose $\overline{D}(\tau|\mathbf{e})$. As a result and with the assumption that nominal process releases occur for all scenario classes, $\overline{D}(\tau|\mathbf{e})$ can be approximated as indicated in Table 3. Example derivations are presented in App. J of Ref. [6] illustrating how the use of disjoint scenario classes to calculate expected dose $\overline{D}(\tau|\mathbf{e})$ in combination with the no significant synergisms assumption leads to the relationships Table 3.

Given the decomposition in Table 3, $\overline{D}(\tau|\mathbf{e})$ can be approximated by (i) approximating $D_N(\tau|\mathbf{a}_N,\mathbf{e}_M)$ and individually approximating the integrals defining the expected incremental doses $\overline{D}_C(\tau|\mathbf{e})$ as indicated in Table 4 (see [6], App. J, for additional details) and then (ii) adding these approximations to obtain an approximation to $\overline{D}(\tau|\mathbf{e})$.

Please cite this article as: Helton JC, et al. Uncertainty and sensitivity analysis in performance assessment for the proposed high-level radioactive waste repository at Yucca Mountain, Nevada. Reliab Eng Syst Safety (2011), doi:10.1016/j.ress.2011.07.002

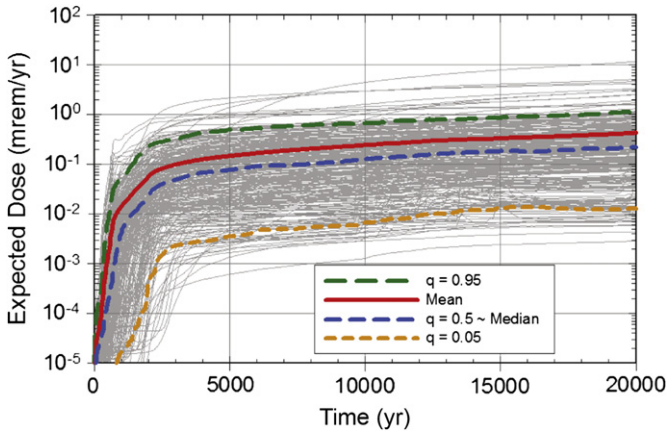

Fig. 2. Expected, mean and median curves for dose to the RMEI for all scenario classes ([6], Fig. K8.1-1[a]).

Table 3
Decomposition of expected dose $\overline{D}(\tau|\mathbf{e})$ into expected incremental doses $\overline{D}_C(\tau|\mathbf{e})$ from individual scenario classes) ([9], Table III and [15], Table 17.3; see [6], Sect. J4.6, for additional discussion).

$$\begin{aligned}\overline{D}(\tau|\mathbf{e}) &= \int_{\mathcal{A}} D(\tau|\mathbf{a},\mathbf{e}_M)d_A(\mathbf{a}|\mathbf{e}_A)\mathrm{d}A \\ &\cong \int_{\mathcal{A}} \left\{ D_N(\tau|\mathbf{a}_N,\mathbf{e}_M) + \sum_{C\in\mathcal{MC}} D_C(\tau|\mathbf{a},\mathbf{e}_M) \right\} d_A(\mathbf{a}|\mathbf{e}_A)\mathrm{d}A \\ &\quad \times \text{with} \begin{cases} D(\tau|\mathbf{a},\mathbf{e}) \cong D_N(\tau|\mathbf{a}_N,\mathbf{e}_M) + \sum_{C\in\mathcal{MC}} D_C(\tau|\mathbf{a},\mathbf{e}_M) \\ \mathcal{MC} = \{EW,ED,II,IE,SG,SF\} \end{cases} \\ &= D_N(\tau|\mathbf{a}_N,\mathbf{e}_M) + \sum_{C\in\mathcal{MC}} \int_{\mathcal{A}} D_C(\tau|\mathbf{a},\mathbf{e}_M)d_A(\mathbf{a}|\mathbf{e}_A)\mathrm{d}A \\ &= D_N(\tau|\mathbf{a}_N,\mathbf{e}_M) + \sum_{C\in\mathcal{MC}} \int_{\mathcal{A}_C} D_C(\tau|\mathbf{a},\mathbf{e}_M)d_A(\mathbf{a}|\mathbf{e}_A)\mathrm{d}A \\ &= D_N(\tau|\mathbf{a}_N,\mathbf{e}_M) + \sum_{C\in\mathcal{MC}} \overline{D}_C(\tau|\mathbf{e})\end{aligned}$$

where $\mathbf{a}_N$ corresponds to the single future associated with the nominal scenario class $\mathcal{A}_N$ in which no disruptions of any kind occur, $D_N(\tau|\mathbf{a}_N,\mathbf{e}_M)$ is the dose to the RMEI that results solely from processes associated with the nominal scenario class, and $D_C(\tau|\mathbf{a},\mathbf{e}_M)$ is the incremental dose to the RMEI that results solely from the effects of the disruptions that result in the future $\mathbf{a}$ being an element of the scenario class (i.e., set) $\mathcal{A}_C$.

Table 4
Integration procedures used to obtain expected incremental dose $\overline{D}_C(\tau|\mathbf{e})$ for individual scenario classes in the 2008 YM PA ([9], Table IV and [15], Table 17.4; see [6], Sects. J5–J8, for additional discussion).

Nominal conditions: $\overline{D}_N(\tau|\mathbf{e})$
- Always zero for [0, 2×10^4 yr] in 2008 YM PA
- Combined with seismic ground motion for [0, 10^6 yr]

Early WP and DS Failures: $\overline{D}_{EW}(\tau|\mathbf{e})$, $\overline{D}_{ED}(\tau|\mathbf{e})$
- Summation of probabilistically weighted results for individual failures

Igneous intrusive events: $\overline{D}_{II}(\tau|\mathbf{e})$
- Quadrature procedure

Igneous eruptive events: $\overline{D}_{IE}(\tau|\mathbf{e})$
- Combined quadrature/Monte Carlo procedure

Seismic ground motion events: $\overline{D}_{SG}(\tau|\mathbf{e})$
- Quadrature procedure for [0, 2×10^4 yr]
- Monte Carlo procedure for [0, 10^6 yr]

Seismic fault displacement events: $\overline{D}_{SF}(\tau|\mathbf{e})$
- Quadrature procedure

The mean dose $\overline{\overline{D}}(\tau)$ and the median dose $Q_{E,0.5}[\overline{D}(\tau|\mathbf{e})]$ are defined by integrals over the set $\mathcal{E}$ of epistemically uncertain analysis inputs as indicated in Eqs. (7) and (8). In the 2008 YM PA, these integrals are approximated with use of a Latin hypercube sample (LHS)

$$\mathbf{e}_i = [\mathbf{e}_{Ai},\mathbf{e}_{Mi}], \quad i = 1,2,\ldots,nLHS, \tag{9}$$

of size $nLHS=300$ generated in consistency with the definition of the probability space $(\mathcal{E}, \mathbb{E}, p_E)$ (i.e., in consistency with the distributions defined for the individual elements of $\mathbf{e}$) [58,59]. Then, $\overline{\overline{D}}(\tau)$ and $p_E[\overline{D}(\tau|\mathbf{e}) \le D]$ are approximated by

$$\overline{\overline{D}}(\tau) \cong \sum_{i=1}^{nLHS} \overline{D}(\tau|\mathbf{e}_i)/nLHS \tag{10}$$

and

$$p_E[\overline{D}(\tau|\mathbf{e}) \le D] \cong \sum_{i=1}^{nLHS} \underline{\delta}_D[\overline{D}(\tau|\mathbf{e}_i)]/nLHS, \tag{11}$$

respectively. Further, this sample can be used in a numerical determination of the quantiles $Q_{E,q}[\overline{D}(\tau|\mathbf{e})]$ for $\overline{D}(\tau|\mathbf{e})$defined in Eq. (8). Analogous approximations to mean and median doses over epistemic uncertainty also exist for the individual scenario classes.

2.5. Disjoint and nondisjoint scenario classes

As used in this presentation, a scenario class is any element of the set $\mathbb{A}$ appearing in the formal definition of the probability space $(\mathcal{A}, \mathbb{A}, p_A)$ for aleatory uncertainty. Specifically, a scenario class is any subset $\mathcal{S}$ of the set $\mathcal{A}$ of possible futures (see Table 1) for which a probability $p_A(\mathcal{S})$ can be defined. This definition, which is consistent with the formal development of probability, allows for both disjoint and nondisjoint scenario classes. Consistent with this, both disjoint and nondisjoint scenario classes have significant roles in the 2008 YM PA.

As recognized by the NRC in the following statement from the YMRP ([19], p. 2.2-133), the calculation of expected dose to the RMEI has a conceptual basis that involves the use of disjoint scenario classes: "The occurrence of scenario classes, included in the calculating the annual dose, sum to one." This statement is consistent with the approximation of the expected dose $\overline{D}(\tau|\mathbf{e})$ defined in Eq. (5) by

$$\overline{D}(\tau|\mathbf{e}) \cong \sum_{i=1}^{nS} D(\tau|\mathbf{a}_i,\mathbf{e}_M)p_A(\mathcal{S}_i|\mathbf{e}_A), \tag{12}$$

where the $\mathcal{S}_i$ are elements of $\mathbb{A}$ (i.e., subsets of $\mathcal{A}$), $\mathcal{S}_i \cap \mathcal{S}_j = \emptyset$ if $i \neq j$, $\cup_i \mathcal{S}_i = \mathcal{A}$, $\mathbf{a}_i \in \mathcal{S}_i$, and $p_A(\mathcal{S}_i|\mathbf{e}_A)$ is the probability of $\mathcal{S}_i$. The preceding approximation to $\overline{D}(\tau|\mathbf{e})$ corresponds to an expected value calculation in the context of the ordered triplet representation for risk $(\mathcal{S}_i, pS_i, \mathbf{cS}_i)$, $i=1, 2,\ldots,nS$, in Eq. (1). Specifically, the sets $\mathcal{S}_i$ are the same, $p_A(\mathcal{S}_i|\mathbf{e}_A)$ corresponds to pS_i, and $D(\tau|\mathbf{a}_i,\mathbf{e}_M)$ corresponds to an element of $\mathbf{cS}_i$.

As indicated in Eq. (12), the calculation of expected dose to the RMEI in the 2008 YM PA can be formally based on the consideration of disjoint scenario classes with probabilities that sum to one. However, in computational practice, the number of disjoint scenario classes required for the sum in Eq. (12) to be a reasonable approximation to $\overline{D}(\tau|\mathbf{e})$ is both large and difficult to determine (e.g., see Ref. [60]). For this reason and with described justification ([6], App. J), the 2008 YM PA approximates $\overline{D}(\tau|\mathbf{e})$ on the basis of the no significant synergisms decomposition indicated in Table 3. This decomposition involves the nondisjoint scenario classes $\mathcal{A}_C$, $C=EW$, ED, II, IE, SG, SF, appearing in Tables 1 and 3. Specifically, the starting integral that defines $\overline{D}(\tau|\mathbf{e})$ in Eq. (5) is predicated on the concept of disjoint scenario

Please cite this article as: Helton JC, et al. Uncertainty and sensitivity analysis in performance assessment for the proposed high-level radioactive waste repository at Yucca Mountain, Nevada. Reliab Eng Syst Safety (2011), doi:10.1016/j.ress.2011.07.002

classes. In particular, the correct place to check for conservation of probability in the determination of $\overline{D}(\tau|\mathbf{e})$ is in the integral definition of $\overline{D}(\tau|\mathbf{e})$ in Eq. (5) rather than after the no significant synergisms assumption has been implemented at the end of Table 3. This decomposition is very beneficial because implementing integrals over the sets $\mathcal{A}_C$ where the effects of only one type of event are considered (see Table 4) is much easier that implementing an integral over the entire set $\mathcal{A}$. This decomposition also facilitates informative uncertainty and sensitivity analyses of the form presented in Sections 4 and 5 and in more detail in Apps. J and K of Ref. [6].

In addition, when scenario class probabilities are requested, it is likely that the desired probabilities are for the nondisjoint scenario classes $\mathcal{A}_C$, $C=EW$, ED, II, IE, SG, SF, or possibly some other collection of nondisjoint scenario classes. In particular, it is probabilities for the nondisjoint scenario classes $\mathcal{A}_C$ that are presented in App. J of Ref. [6]. For example, if probability of early WP failure is under consideration, then most likely $p_A(\mathcal{A}_{EW}|\mathbf{e}_A)$ rather than $p_A(\{\mathbf{a}|nEW>0,\ nED=nII=nIE=nSG=nSF=0\}|\mathbf{e}_A)$ is the probability of interest. Specifically, the $p_A(\mathcal{A}_{EW}|\mathbf{e}_A)$ is the probability that one or more early WP failures occur while $p_A(\{\mathbf{a}|nEW>0,\ nED=nII=nIE=nSG=nSF=0\}|\mathbf{e}_A)$ is the probability that one or more early WP failures occur and also that no other failures of any other type occur; this latter probability is significantly affected by the indicated nonoccurrence assumptions and effectively provides no information on the likelihood of early WP failures.

3. Uncertainty and sensitivity analysis techniques

The importance of an appropriate assessment of the uncertainty present in PAs for the proposed YM repository has been strongly emphasized by the NRC (e.g., Quotes (NRC4) and (NRC5)). As a result, uncertainty analysis and sensitivity analysis are important parts of the 2008 YM PA, where uncertainty analysis designates the determination of the uncertainty in analysis results that derives from uncertainty in analysis inputs and sensitivity analysis designates the determination of the contributions of individual uncertain analysis inputs to the uncertainty in analysis results.

As described in Section 2.2 and in more detail in an extensive analysis report ([6], App. J), the conceptual structure and computational organization of the 2008 YM PA involves three basic entities: EN1, a characterization of the uncertainty in the occurrence of future events that could affect the performance of the repository; EN2, models for predicting the physical behavior and evolution of the repository; and EN3, a characterization of the uncertainty associated with analysis inputs that have fixed but imprecisely known values. In the context of the preceding entities, uncertainty analysis involves the determination of the uncertainty in predictions by the model corresponding to EN2 that derives from the uncertainty in analysis inputs characterized by the probability space $(\mathcal{E}, \mathbb{E}, p_E)$ corresponding to EN3. Further, this determination is made for either (i) results conditional on the occurrence of specific futures contained in the set $\mathcal{A}$ or (ii) expected results based on the probability space $(\mathcal{A}, \mathbb{A}, p_A)$ and obtained by integrating over the set $\mathcal{A}$. Similarly, sensitivity analysis involves the determination of the effects of individual variables contained in elements $\mathbf{e}$ of $\mathcal{E}$ on results of the form just indicated.

The primary emphasis of Section 4 of this paper is on uncertainty and sensitivity analysis for results conditional on the occurrence of specific futures contained in the set $\mathcal{A}$. Then, Section 5 considers uncertainty and sensitivity analysis for expected results based on the probability space $(\mathcal{A}, \mathbb{A}, p_A)$ and obtained by integrating over the set $\mathcal{A}$.

Conceptually, the models comprising component EN2 of the 2008 YM PA can be represented by a function

$$\mathbf{y}(\tau|\mathbf{a},\mathbf{e}) = \mathbf{f}(\tau|\mathbf{a},\mathbf{e}), \tag{13}$$

where $\mathbf{a}=[a_1,a_2,\ldots,a_{nA}]$ is an element (i.e., future) contained in $\mathcal{A}$ (see Eq. (2) and Table 1), $\mathbf{e}=[e_1,e_2,\ldots,e_{nE}]$ is an element of $\mathcal{E}$ (see Eq. (4) and Table 2), and

$$\mathbf{y}(\tau|\mathbf{a},\mathbf{e}) = [y_1(\tau|\mathbf{a},\mathbf{e}),y_2(\tau|\mathbf{a},\mathbf{e}),\ldots,y_{nY}(\tau|\mathbf{a},\mathbf{e})] \tag{14}$$

is the value of the function $\mathrm{f}(\tau|\mathbf{a},\mathbf{e})$ at time τ (see Ref. [6], Chap. 6, and Refs. [42–44]). In general, the dimensions nA and nY of $\mathbf{a}$ and $\mathbf{y}(\tau|\mathbf{a},\mathbf{e})$ can be quite large with the elements of $\mathbf{y}(\tau|\mathbf{a},\mathbf{e})$ corresponding to results obtained from individual models of the form indicated in Fig. 1. The dimension nE of $\mathbf{e}$ in the 2008 YM PA is 392; however, most elements of $\mathbf{y}(\tau|\mathbf{a},\mathbf{e})$are potentially affected by only a subset of the variables contained in e. The elements of $\mathrm{y}(\tau|\mathbf{a},\mathbf{e})$ include both physical properties of the YM system (e.g., temperature, pH, radionuclide release rates, …) and quantities involving dose to the RMEI (e.g., the doses $D_N(\tau|\mathbf{a}_N,\mathbf{e}$, $D_C(\tau|\mathbf{a},\mathbf{e})$ and $D(\tau|\mathrm{a},\mathbf{e})$ indicated in Table 3.

The uncertainty associated with $\mathbf{e}$ is characterized by a sequence of distributions

$$D_1,D_2,\ldots,D_{nE}, \tag{15}$$

where D_j is the distribution assigned to the element e_j of $\mathbf{e}$ (i.e., see the variables and distributions indicated in Table 2 and given in full in Tables K3-1, K3-2 and K3-3 of Ref. [6]). Correlations and other restrictions are also assumed to exist between some variables. The distributions indicated in Eq. (15) and any associated restrictions characterize epistemic uncertainty and, in effect, define the probability space $(\mathcal{E}, \mathbb{E}, p_E)$.

As described in conjunction with Eq. (9), Latin hypercube sampling is used to propagate the uncertainty characterized by the distributions indicated in Eq. (15) in the 2008 YM PA. Specifically, an LHS

$$\mathbf{e}_i = [e_{i1},e_{i2},\cdots,e_{i,nE}],\quad i=1,2,\cdots,nLHS, \tag{16}$$

of size $nLHS=300$ is generated from the possible values for $\mathbf{e}$ (i.e., form the set $\mathcal{E}$). Then, the function $\mathbf{f}(\tau|\mathbf{a},\mathbf{e})$ is evaluated for each element e_i of the LHS indicated in Eq. (16). This creates a mapping

$$[\mathbf{e}_i,\mathbf{y}(\tau|\mathbf{a},\mathbf{e}_i)],\quad i=1,2,\cdots,nLHS=300, \tag{17}$$

from uncertain analysis inputs to uncertain analysis results. In practice, the indicated mapping is generated many times for different values of $\mathbf{a}$ for the calculation of each of the doses $D_C(\tau|\mathbf{a},\mathbf{e})$ indicated in Table 3.

Once generated, the mapping in Eq. (17) provides the basis for both uncertainty analysis and sensitivity analysis. Specifically, each sample element has a weight (i.e., a probability in common but incorrect usage) of $1/nLHS=1/300$ that can be used to estimate CDFs and complementary cumulative distribution functions (CCDFs) that summarize the uncertainty in analysis results. In addition, expected values (i.e., means) and various quantiles can also be obtained and used to summarize the uncertainty in analysis results. Or, most simply, the spread of the results obtained for individual elements of $\mathbf{y}(\tau|\mathbf{a},\mathbf{e})$ can be presented.

Sensitivity analysis results can be obtained by exploring the mapping between analysis inputs and analysis results in Eq. (17) with a variety of procedures. The simplest is to examine scatterplots that graphically show the relationships between an element of $\mathbf{y}(\tau|\mathbf{a},\mathbf{e})$ and individual elements of $\mathbf{e}$ (i.e., plots of points of the form $[e_{ij},\ y_k(\tau|\mathbf{a},\mathbf{e}_i)]$, $i=1,2,\ldots,nLHS$, for individual elements e_j and $y_k(\tau|\mathbf{a},\mathbf{e}_i)$ of $\mathbf{e}$ and $\mathbf{y}(\tau|\mathbf{a},\mathbf{e})$, respectively) ([61], Section 6.6.1). More complex analyses involve the use of partial correlation coefficients (PCCs) and stepwise regression analyses to assess the relationships between analysis inputs and analysis results

Please cite this article as: Helton JC, et al. Uncertainty and sensitivity analysis in performance assessment for the proposed high-level radioactive waste repository at Yucca Mountain, Nevada. Reliab Eng Syst Safety (2011), doi:10.1016/j.ress.2011.07.002

([61], Sections 6.6.2–6.6.5). With stepwise regression analysis, variable importance is indicated by the order of selection in the stepwise process, the incremental increase in R^2 values as variables are added to the regression model, and the standardized regression coefficients (SRCs) in the final regression model. A SRC provides a measure of the fraction of the uncertainty in an analysis RESULT accounted for by a given analysis input; in contrast, a PCC provides a measure of the strength of the linear relationship between an analysis result and a given analysis input after the linear effects of all other analysis inputs have been removed. When nonlinear relationships are present, analyses are often performed with rank transformed data ([61], Section 6.6.6, [62]), which results in partial rank correlation coefficients (PRCCs) and standardized rank regression coefficients (SRRCs) rather than PCCs and SRCs. Most of the sensitivity analyses carried out as part of the 2008 YM PA were performed with rank-transformed data due to the effectiveness of this transformation in facilitating informative sensitivity analyses in the presence of (i) monotonic relationships between variables and (ii) the distorting effects of extreme outliers.

Detailed descriptions of the sensitivity analysis procedures used in the 2008 YM PA are available in Refs. [59,61,63]. Additional background information is available in references cited in Refs. [59,61,63] and also in Refs. [64–70].

The approach to uncertainty analysis and sensitivity analysis employing Latin hypercube sampling and an exploration of the resultant mapping between uncertain analysis inputs and resultant analysis outcomes was adopted for use in the 2008 YM PA on the basis of the requirements and properties of this particular analysis. Considerations that led to this adoption include (i) regulatory requirements to propagate and display the effects of uncertainty and also to determine both expected values over aleatory uncertainty conditional on specific realizations of epistemic uncertainty and expected values over aleatory uncertainty and epistemic uncertainty, (ii) the need to propagate epistemic uncertainty through a sequence of computationally demanding models with a limited number of model evaluations, (iii) the need to decompose and recompose calculations in an effective manner to enhance computational efficiency and analysis insights, (iv) the need to determine uncertainty and sensitivity analysis results for 100's of time-dependent analysis outcomes without excessive demands on human and computational time, and (v) a desire for the uncertainty and sensitivity procedures in use to be an important and effective component of analysis verification.

There are a number of approaches to uncertainty and sensitivity analysis in addition to the sampling-based approach used in the 2008 YM PA, including differential analysis [71–80], response surface methodology [81–87], moment independent methods [88–91], and variance decomposition procedures [92–99]. Overviews of these approaches are available in several reviews [68,100–110]. However, given the scale of the 2008 YM PA and the need for analysis flexibility and computational efficiency, it was felt that the sampling-based approach to uncertainty and sensitivity analysis selected for use is the most appropriate choice from the extensive universe of established techniques for uncertainty and sensitivity analysis. This choice is reinforced by the successful use of similar sampling-based procedures in the NRC's reassessment of the risk from commercial nuclear power plants (i.e., the NUREG-1150 analyses) [111–117] and the DOE's PA in support of a successful compliance certification application for the Waste Isolation Pilot Plant [118–121].

4. Uncertainty and sensitivity analysis for physical processes

4.1. Nominal scenario class $\mathcal{A}_N$

A large number of analysis results are considered in the uncertainty and sensitivity analyses for the nominal scenario class $\mathcal{A}_N$ (Table 5). The variables indicated in Table 5 correspond to a subset of the variables $y_k(\tau|\mathbf{a},\mathbf{e})$ that comprise the elements of $\mathbf{y}(\tau|\mathbf{a},\mathbf{e})$ in Eq. (14). Of these variables, the number of failed commercial spent nuclear fuel WPs in percolation bin 3 (*NCSFL*) is used as an initial example for illustration (Fig. 3). The element $\mathbf{a}_N$ of $\mathcal{A}$ under consideration corresponds to the future in which no disruptions of any kind take place.

Table 5
Examples of 11 of the 32 time-dependent results analyzed for the nominal scenario class ([10], Table I; see [6], Table K4.1-1, for additional details).

BACSFLAD: Average breached area (m^2) on failed commercial spent nuclear fuel (CSNF) WPs under dripping conditions ([6], Figs. K.4.2-6, K.4.2-7)
DOSTOT: Dose to RMEI (mrem/yr) from all radioactive species ([6], Figs. K4.5-1, K4.5-2, K4.5-3)
DSFLTM: Drip shield failure time (yr) ([6], Fig. K.4.2-1)
ISCSINAD: Ionic strength (molal) in the invert beneath the WP for CSNF WPs under dripping conditions ([6], Figs. K.4.3-9, K.4.3-11)
NCDFL: Number of failed codisposed spent nuclear fuel (CDSP) WPs ([6], Fig. K.4.2-2)
NCSFL: Number of failed CSNF WPs ([6], Figs. K.2-1, K.4.2-3)
NCSFLAD: Number of failed CSNF WPs under dripping conditions ([6], Figs. K.4.2-4, K.4.2-5)
NCSFLND: Number of failed CSNF WPs under nondripping conditions ([6], Figs. K.4.2-4, K.4.2-5)
PCO2CSIA: Partial pressure of CO_2 (bars) in the invert for CSNF WPs under dripping conditions ([6], Figs. K.4.3-7, K.4.3-8)
PHCSINAD: pH in the invert beneath the WP for CSNF WPs under dripping conditions ([6], Figs. K.4.3-12, K.4.3-13)
RHCDINV: Relative humidity for CDSP WPs in the invert beneath the WP ([6], Figs. K.4.3-6)

The uncertainty in the time-dependent values for *NCSFL* is shown by the 300 curves in Fig. 3a, with a single curve resulting for each of the LHS elements $\mathbf{e}_i$ in Eq. (16). Sensitivity analysis results based on PRCCs and stepwise rank regression are presented in Fig. 3b and c. Specifically, Fig. 3b and other similar figures in this presentation display PRCCs for the six variables with the largest maximum PRCCs in absolute value over the time interval under consideration and correspondingly order the associated variables in the internal figure label subject to the constraint that the indicated maximum value must be at least 0.3 for a variable and its PRCC to be included in a figure (see Ref. [61], Sections 6.6.4 and 6.6.6, for additional information on PRCCs), and the stepwise rank regression in Fig. 3c used a significance level of $\alpha=0.01$ to terminate the stepwise selection process (see Ref. [61], Sections 6.6.2–6.6.6, for additional information on stepwise rank regression). In the analyses in Fig. 3b and c, the dominant variable with respect to the uncertainty in *NCSFL* is *WDGCA22* (see Table 2 for variable definitions), with *NCSFL* tending to decrease as *WDGCA22* increases. This effect results because of the role that increasing *WDGCA22* plays in decreasing the rate of general corrosion. The strong effect of *WDGCA22* on *NCSFL* can be seen in the scatterplot in Fig. 3d. After *WDGCA22*, a number of additional variables are identified as having small effects on *NCSFL*.

As another example, analyses for dose from all radionuclides for the nominal scenario class $\mathcal{A}_N$ (i.e., $D_N(\tau|\mathbf{e}_M)$, or equivalently, *DOSTOT*) are presented in Fig. 4. The uncertainty in the time-dependent values for *DOSTOT* is shown by the 300 curves in Fig. 4a, with a single curve resulting for each of the LHS elements $\mathbf{e}_i$ in Eq. (16). Sensitivity analysis results based on PRCCs are presented in Fig. 4b. The dominant variables with respect to the uncertainty in *DOSTOT* are *WDGCA22* and *WDZOLID* (see Table 2 for variable definitions), with *DOSTOT* tending to decrease as *WDGCA22* increases and to increase as *WDZOLID* as increases. These effects result because increasing *WDGCA22* decreases WP failures due to general corrosion (see Fig. 3) and increasing *WDZOLID* increases corrosion-induced failures of welds at the WP lids.

Please cite this article as: Helton JC, et al. Uncertainty and sensitivity analysis in performance assessment for the proposed high-level radioactive waste repository at Yucca Mountain, Nevada. Reliab Eng Syst Safety (2011), doi:10.1016/j.ress.2011.07.002

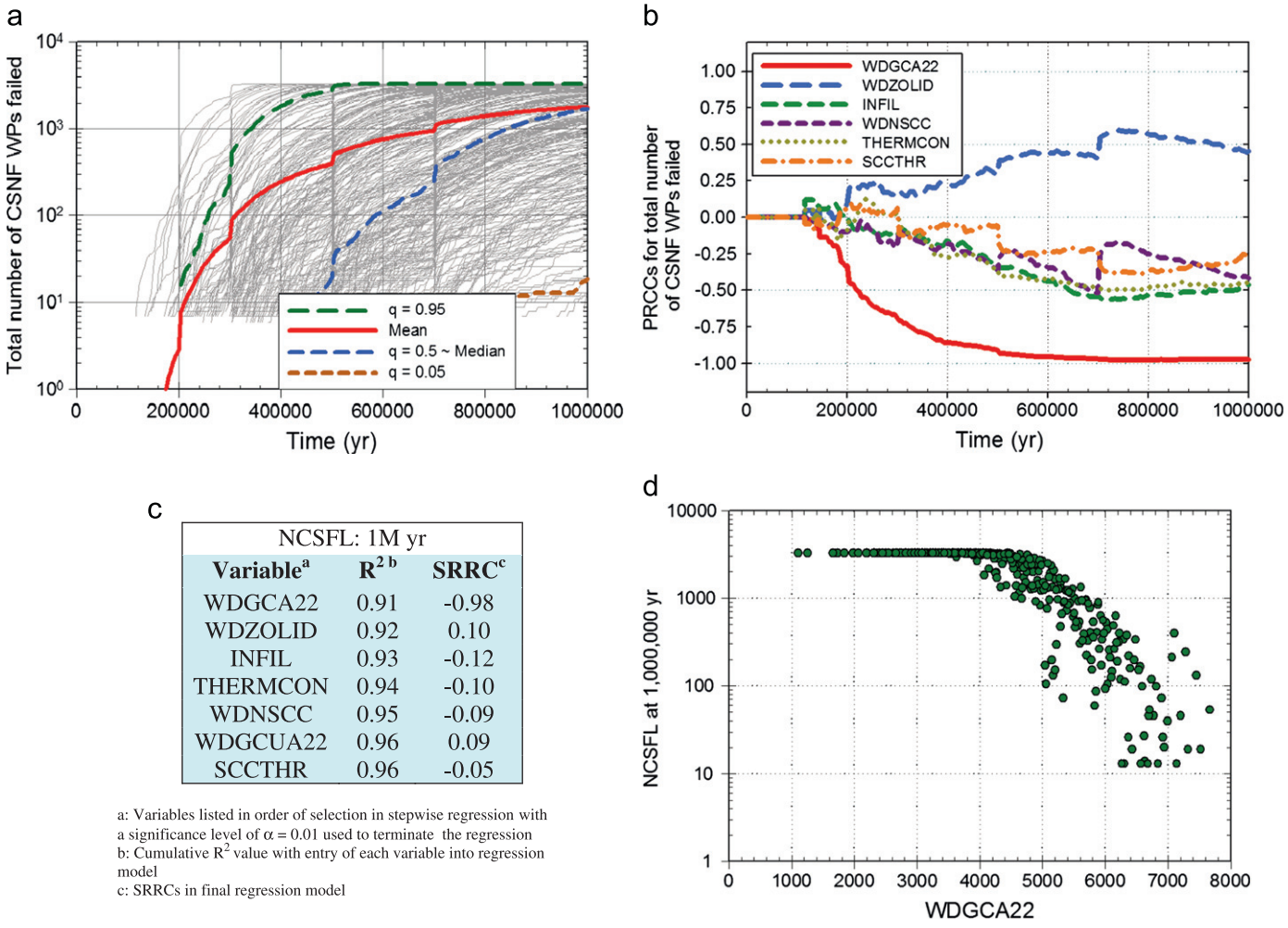

c

NCSFL: 1M yr		
Variable[a]	**R^{2} [b]**	**SRRC[c]**
WDGCA22	0.91	-0.98
WDZOLID	0.92	0.10
INFIL	0.93	-0.12
THERMCON	0.94	-0.10
WDNSCC	0.95	-0.09
WDGCUA22	0.96	0.09
SCCTHR	0.96	-0.05

a: Variables listed in order of selection in stepwise regression with a significance level of $\alpha = 0.01$ used to terminate the regression
b: Cumulative R^2 value with entry of each variable into regression model
c: SRRCs in final regression model

Fig. 3. Uncertainty and sensitivity analysis results for total number of CSNF WPs failed for the nominal scenario class (*NCSFL*): (a) *NCSFL* for all (i.e., 300) sample elements, (b) PRCCs for *NCSFL*, (c) stepwise rank regression analysis for *NCSFL* at 10^6 yr, and (d) scatterplot for (*WDGCA22*, *NCSFL*) at 10^6 yr ([10], Fig. 1, and [15], Fig. 17.6; see [6], Fig. K2-1, for additional discussion).

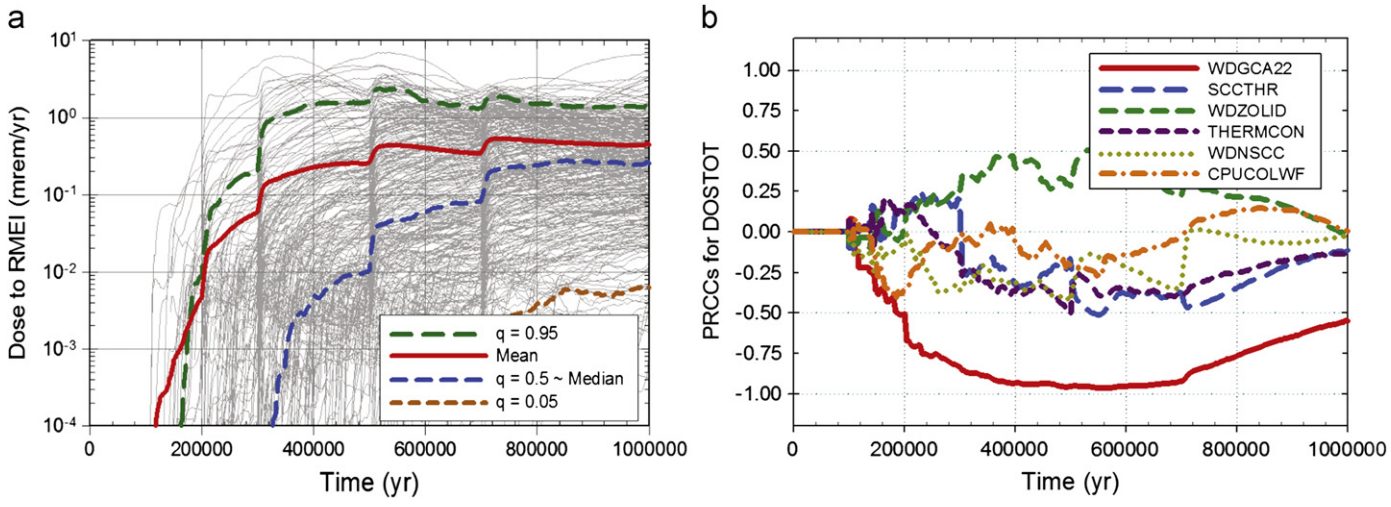

Fig. 4. Uncertainty and sensitivity analysis results for dose to the RMEI (mrem/yr) for the nominal scenario class (i.e., for $D_N(\tau|a_N,e_M)$ as defined in Table 3 and represented by *DOSTOT*): (a) *DOSTOT* for all (i.e., 300) sample elements, and (b) PRCCs for *DOSTOT* ([10], Fig. 2 and [6], Fig. K4.5-1[a]).

Analyses similar to those presented in Figs. 3 and 4 were carried out for the nominal scenario class for 32 analysis results, of which 11 are indicated in Table 5 ([6], Section K4).

Stepwise rank regression results of the form shown in Fig. 3c contain more detailed information than is provided by PRCCs at a specific point in time. However, the display of stepwise regression

results obtained at a sequence of times results in a much bulkier presentation than the display of time-dependent PRCCs as done in Fig. 3b. Given this difference, this presentation uses a display format with PRCCs of the form shown in Fig. 4 so that paired uncertainty and sensitivity analysis results can be shown for a variety of important analysis outcomes from the 2008 YM PA in a reasonable amount of space. However, stepwise rank regression results for the variables analyzed with PRCCs in this presentation can be found in App. K of Ref. [6]. An alternative to the display of time-dependent PRCCs is to display time-dependent plots of SRRCs. As indicated in Section 3, PCCs and SRCs display related, but different, aspects of the relationships between variables. However, when the sampled variables are independent, a ranking of variable importance on the basis of the absolute values of PCCs is the same as a ranking of variable importance on the basis of the absolute values of SRCs (see Ref. [61], Section 6.6.4). Thus, displays of PCCs and displays of SRCs give the same general impressions of variable importance. For the 2008 YM PA, the choice was made to display PRCCs rather than SRRCs because PRCCs tend to be more spread out than SRRCs and thus result in plots that are easier to read. So that the information contained in SRRCs and associated stepwise regression analyses was not lost, the 2008 YM PA also presented extensive results of the form shown in Fig. 3c in App. K of Ref. [6].

4.2. Igneous intrusive scenario class $\mathcal{A}_{II}$

As for the nominal scenario class, a large number of analysis results are considered in the uncertainty and sensitivity analyses for the igneous intrusive scenario class $\mathcal{A}_{II}$ (Table 6). The variables indicated in Table 6 correspond to a subset of the variables $y_k(\tau|\mathbf{a},\mathbf{e})$ that comprise the elements of $\mathbf{y}(\tau|\mathbf{a},\mathbf{e})$ in Eq. (14). As examples, this section considers the movement of ^{237}Np through the repository system and the dose to the RMEI that results from this movement. The specific element $\mathbf{a}$ of $\mathcal{A}$ under consideration corresponds to a single igneous intrusive event that occurs at 10 yr after repository closure and damages all WPs in the repository, and the results selected for presentation are *ESNP237*, *UZNP237*, *SZNP237* and *DONP237* as defined in Table 6.

The uncertainty in the time-dependent values for *ESNP237* and *UZNP237* is shown by the 300 curves in Fig. 5a and c, with a single curve resulting for each of the LHS elements $\mathbf{e}_i$ in Eq. (16). Sensitivity analysis results for *ESNP237* based on PRCCs are presented in Fig. 5b and indicate (i) positive effects for *EP1NPO2, INFIL, DELPPCO2* and *EP1LOWAM*, (ii) a negative effect for *PHCSS*, and (iii) a very early positive effect for *THERMCON* (see Table 2 for variable definitions). The indicated effects result because (i) increasing *EP1NPO2* and *DELPPCO2* increases the solubility of neptunium, (ii) increasing *INFIL* increases water flow through the engineered barrier system (EBS), (iii) increasing *EP1LOWAM* increases the solubility of ^{241}Am, which is a parent of ^{237}Np, (iv) increasing *PHCSS* decreases the solubility of neptunium, and (v) increasing *THERMCON* decreases the time required for the repository to reach below-boiling temperatures for water and thereby facilitates early radionuclide releases. The general increase in *UZNP237* at 10^4 yr results from a climate change imposed at that time for all sample elements ([6], Section 6.3.1). The small amplitude variability present in curves for *UZNP237* for individual sample elements results from the use of a particle tracking method for determining transport through the unsaturated zone (UZ) ([6], Section 6.3.9).

The similarity of the releases *ESNP237* and *UZNP237* for ^{237}Np is apparent in Fig. 5a and c and indicates that processes in the UZ have limited effect on the uncertainty in the movement of ^{237}Np. In general, the cumulative mass of ^{237}Np exiting the UZ (i.e., *UZNP237C*) is approximately half of the mass entering the UZ (i.e., *ESNP237C*) as indicated in the scatterplot in Fig. 5d. As a result, the PRCCs for *UZNP237* are essentially the same as the PRCCs for *ESNP237,* and thus show same relationships as shown in Fig. 5b for the PRCCs for *ESPN237*. The retention of ^{237}Np in the UZ is generally due to diffusion of radionuclides into the rock matrix.

The uncertainty in the time-dependent values for *SZNP237* and *DONP237* is shown by the 300 curves in Fig. 6a and c. Unlike the UZ, the saturated zone (SZ) can have a significant effect on the movement of ^{237}Np to the location of the RMEI (Fig. 7). In particular, travel time through the SZ may be significantly longer than 2×10^4 yr.

Sensitivity analysis results for *SZNP237* based on PRCCs are presented in Fig. 6b and indicate (i) positive effects for *SZGWSDM, EP1NPO2* and *INFIL*, (ii) a negative effect for *PHCSS*, and (iii) an early positive effect *THERMCON* and an early negative effect for *SZFIPOVO* (see Table 2 for variable definitions). The indicated effects for *EP1NPO2*, *INFIL*, and *PHCSS* derive from their previously discussed effects on release from the EBS. The positive effect associated with *SZGWSDM* results from increasing water flow in the SZ, and the early negative effect associated with *SZFIPOVO* results from slowing the initial movement of released radionuclides in the SZ.

The comparison of *SZNP237* and *DONP237* at 10^4 yr in the scatterplot in Fig. 6d shows that the uncertainty in *SZNP237* dominates the uncertainty in *DONP237*. This means that the PRCCs for *DONP237* are essentially the same as the PRCCs for *SZNP237*, and indicate the same relationships as shown in Fig. 6b for the PRCCs for *SZPN237*.

Analyses similar to those presented in Figs. 5–7 were carried out for 49 results for the igneous scenario class, of which 7 are indicated in Table 6 ([6], Section K6).

Table 6
Examples of 7 of the 49 time-dependent results analyzed for the igneous intrusive scenario class ([10], Table III; see [6], Table K6.1-1, for additional information).

DONP237: Dose to RMEI (mrem/yr) from dissolved ^{237}Np ([6], Figs. K.6.6.1-5, K.6.6.1-6, K.6.6.2-3)
ESNP237: Release rate (g/yr) for the movement of dissolved ^{237}Np from the engineered barrier system (EBS) to the unsaturated zone (UZ) ([6], Figs. K.6.3.1-5, K.6.3.1-6, K.6.3.2-3)
ESNP237C: Cumulative release (g) for the movement of dissolved ^{237}Np from the EBS to the UZ ([6], Figs. K.6.3.1-5, K.6.3.1-6, K.6.3.2-3, K.6.4.1-9)
SZNP237: Release rate (g/yr) for the movement of dissolved ^{237}Np across a subsurface plane at the location of the RMEI ([6], Figs. K.6.5.1-7, K.6.5.1-8, K.6.5.2-3)
SZNP237C: Cumulative release (g) for the movement of dissolved ^{237}Np across a subsurface plane at the location of the RMEI ([6], Figs. K.6.5.1-7, K.6.5.1-8, K.6.5.1-9, K.6.5.2-3)
UZNP237: Release rate (g/yr) for the movement of dissolved ^{237}Np from the UZ to the saturated zone (SZ) ([6], Figs. K.6.4.1-7, K.6.4.1-8)
UZNP237C: Cumulative release (g) for the movement of dissolved ^{237}Np from the UZ to the SZ ([6], Figs. K.6.4.1-7, K.6.4.1-8, K.6.4.1-9, K.6.5.1-9)

4.3. Additional scenario classes

Example uncertainty and sensitivity analysis results have been presented for the nominal scenario class $\mathcal{A}_N$ and the igneous intrusive scenario class $\mathcal{A}_{II}$. In addition, extensive uncertainty and sensitivity analyses were also carried out as part of the 2008 YM PA for the early WP failure scenario class $\mathcal{A}_{EW}$, the early DS failure scenario class $\mathcal{A}_{ED}$, the igneous eruptive scenario class $\mathcal{A}_{IE}$, the seismic ground motion scenario class $\mathcal{A}_{SG}$, and the seismic fault displacement scenario class $\mathcal{A}_{SF}$. In consistency with the regulatory requirements discussed in Section 2.1, two different time periods were considered for the definition of the sample space $\mathcal{A}$ for aleatory uncertainty in performing these analyses: $[0, 2 \times 10^4$ yr]

Please cite this article as: Helton JC, et al. Uncertainty and sensitivity analysis in performance assessment for the proposed high-level radioactive waste repository at Yucca Mountain, Nevada. Reliab Eng Syst Safety (2011), doi:10.1016/j.ress.2011.07.002

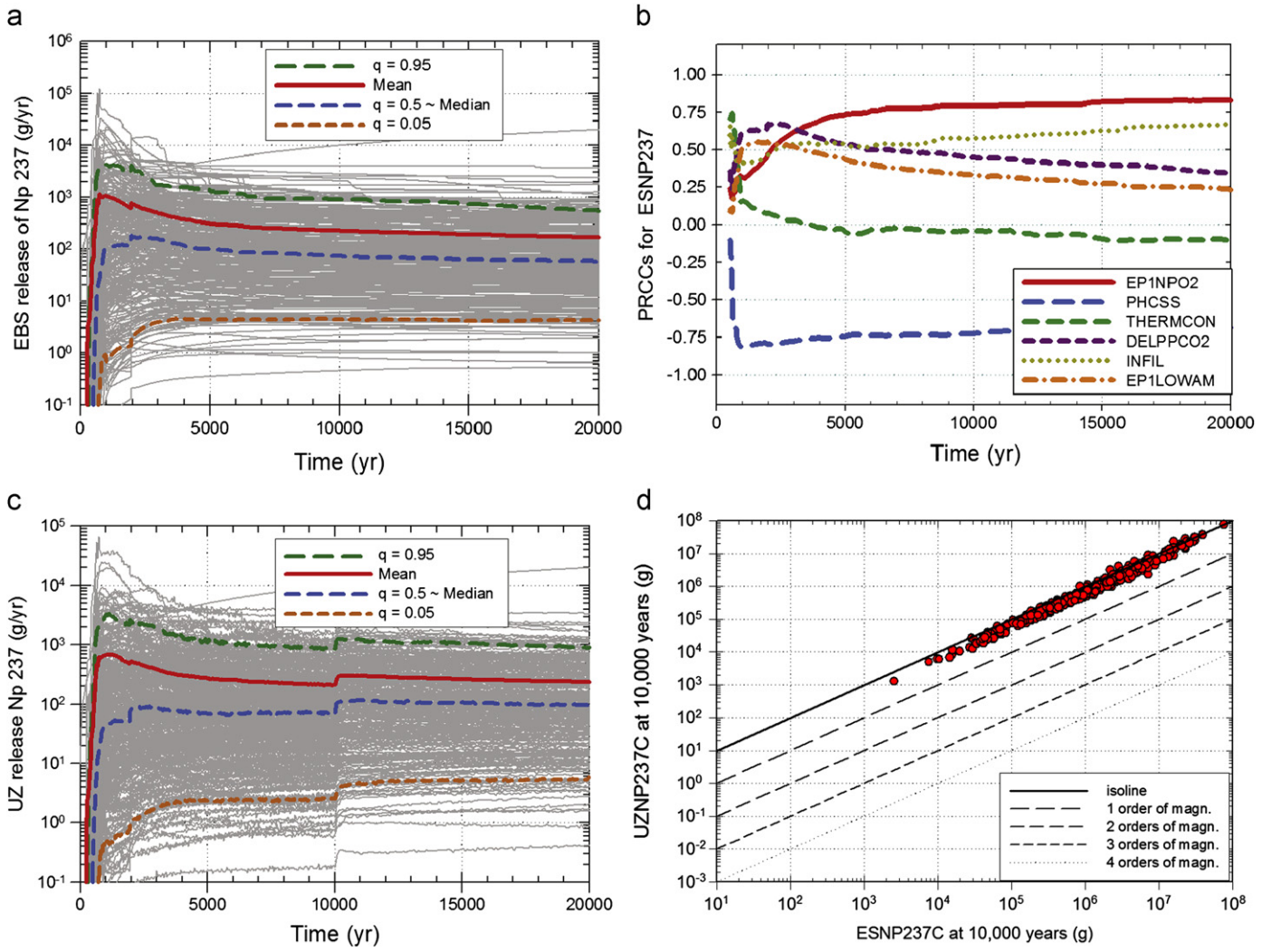

Fig. 5. Uncertainty and sensitivity analysis results for *ESNP237* and *UZNP237* for an igneous intrusive event at 10 yr that damages all WPs in the repository: (a) *ESNP237* for all (i.e., 300) sample elements, (b) PRCCs for *ESNP237*, (c) *UZNP237* for all (i.e., 300) sample elements, and (d) scatterplot for (*ESNP237C*, *UZNP237C*) at 10^4 yr ([10], Fig. 3 and [6], Figs. K6.3.1-5, K6.4.1-7, and K6.4.1-9).

and [0, 10^6 yr]. The results of these analyses are presented in Apps. J and K of Ref. [6].

5. Uncertainty and sensitivity analysis for expected dose

5.1. Early failure scenario classes

As indicated in Table 1, two early failure scenario classes are considered in the 2008 YM PA: the early DS failure scenario class $\mathcal{A}_{ED}$ and the early WP failure scenario class $\mathcal{A}_{EW}$. The possible occurrences of early DS failures and early WP failures are modeled with binomial probability distributions with defining parameters *PROBDSEF* and *PROBWPEF* (see Table 2). The individual DS failure probability *PROBDSEF* applies to all DSs in the repository. Similarly, the individual WP failure probability *PROBWPEF* applies to all WPs in the repository. As modeled, early failures of DSs and WPs occur at repository closure. Further, WPs under early failed DSs are assumed to quickly and completely fail under dripping conditions and to experience no failure under nondripping conditions, and DSs above early failed WPs are assumed to remain intact. However, transport of radionuclides from the affected WPs depends on environmental conditions such as the relative humidity in the affected WPs and the presence of drift seepage ([6], Section 6.3.8, [42]).

The time-dependent expected doses to the RMEI from early DS failure, $\overline{D}_{ED}(\tau|\mathbf{e}_i)$, and early WP failure, $\overline{D}_{EW}(\tau|\mathbf{e}_i)$, for the individual LHS elements $\mathbf{e}_i$, i=1,2,…,300, are shown in Fig. 8a and c. Nonzero values for $\overline{D}_{ED}(\tau|\mathbf{e}_i)$ begin within 2000 years after repository closure (Fig. 8a), with expected dose to the RMEI rising to a sharp initial peak due primarily to advective transport of radionuclides such as ^{99}Tc that are modeled as highly soluble and non-sorbing and then gradually declining to sustained values that are determined by the rates of waste form degradation, radionuclide decay, and radionuclide transport through the engineered and natural barriers. Similarly, nonzero values for $\overline{D}_{EW}(\tau|\mathbf{e}_i)$ begin within 2000 years after repository closure (Fig. 8c), followed by sudden increases in $\overline{D}_{EW}(\tau|\mathbf{e}_i)$ starting at approximately 10^4 yr. These increases correspond to the arrival of radionuclides from early-failed commercial spent nuclear fuel (CSNF) WPs. Because CSNF WPs are in general hotter than co-disposed (CDSP) WPs, formation of continuous liquid pathways occurs later ([6], Section 6.3.8, [42]), delaying release of radionuclides from CSNF WPs. This behavior does not occur for early DS failure due to the associated assumption of completely failed WPs experiencing dripping conditions.

Please cite this article as: Helton JC, et al. Uncertainty and sensitivity analysis in performance assessment for the proposed high-level radioactive waste repository at Yucca Mountain, Nevada. Reliab Eng Syst Safety (2011), doi:10.1016/j.ress.2011.07.002

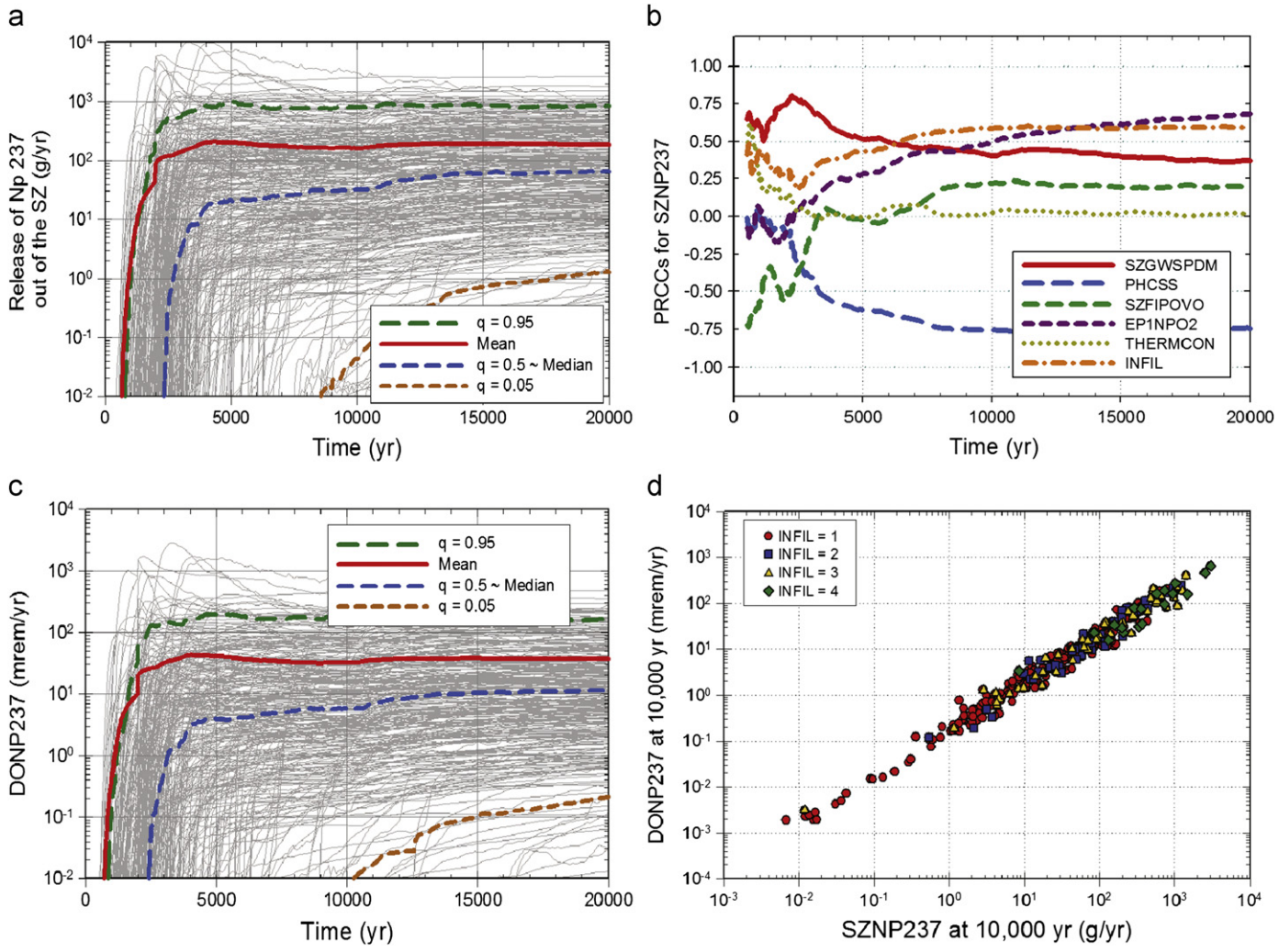

Fig. 6. Uncertainty and sensitivity analysis results for *SZNP237* and *DONP237* for an igneous intrusive event at 10 yr that damages all WPs in the repository: (a) *SZNP237* for all (i.e., 300) sample elements, (b) PRCCs for *SZNP237*, (c) *DONP237* for all (i.e., 300) sample elements, and (d) scatterplot for (*SZNP237*, *DONP237*) at 10^4 yr ([10], Fig. 4 and [6], Figs. K6.5.1-7, K6.6.1-5 and K6.6.1-6).

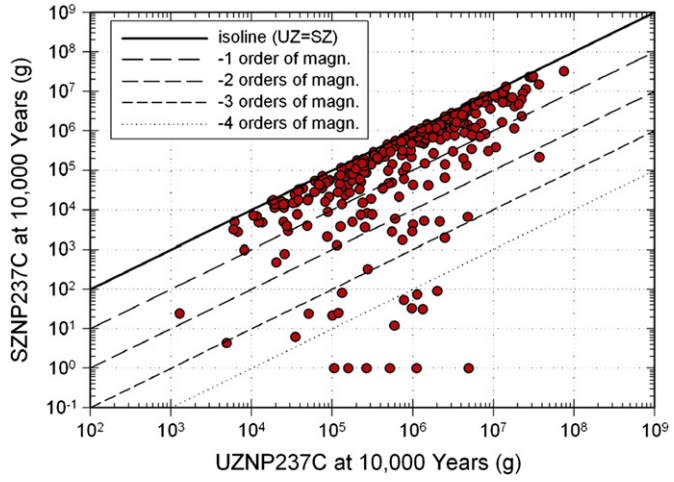

Fig. 7. Scatterplot for (*UZNP237C*, *SZNP237C*) at 10^4 yr for an igneous intrusive event at 10 yr that damages all WPs in the repository ([10], Fig. 5 and [6], Fig.K6.5.1-9).

As shown by the spread of the individual curves, considerable uncertainty exists with respect to the values for $\overline{D}_{ED}(\tau|\mathbf{e}_i)$ and $\overline{D}_{EW}(\tau|\mathbf{e}_i)$. Sensitivity analyses for $\overline{D}_{ED}(\tau|\mathbf{e}_i)$ and $\overline{D}_{EW}(\tau|\mathbf{e}_i)$ based on PRCCs are presented in Fig. 8b and d (see Table 2 for definitions of individual variables). The dominant variables with respect to the uncertainty in $\overline{D}_{ED}(\tau|\mathbf{e})$ and $\overline{D}_{EW}(\tau|\mathbf{e})$ are *PROBDSEF* and *PROBWPEF*, respectively, with $\overline{D}_{ED}(\tau|\mathbf{e})$ and $\overline{D}_{EW}(\tau|\mathbf{e})$ increasing as *PROBDSEF* and *PROBWPEF* increase as a consequence of increasing numbers of early failures. After *PROBDSEF* and *PROBWPEF*, the PRCCs indicate smaller effects for a number of additional variables that influence the movement of water through the engineered and natural barriers of the repository system.

5.2. Igneous scenario classes

Two igneous scenario classes are considered in the 2008 YM PA: the igneous intrusive scenario class $\mathcal{A}_{II}$ and the igneous eruptive scenario class $\mathcal{A}_{IE}$ (Table 1). The occurrence of igneous intrusive events and igneous eruptive events are modeled by Poisson processes with rates defined by *IGRATE* and *IGERATE* (see Table 2). Further, an igneous intrusion event is assumed to destroy all WPs in the repository ([6], Section 6.5, [44]), and an igneous eruptive event ejects the contents of a small number of WPs into the atmosphere ([6], Section 6.5 [44]). The time-dependent expected doses to the RMEI from igneous intrusions, $\overline{D}_{II}(\tau|\mathbf{e}_i)$, and from igneous eruptions, $\overline{D}_{IE}(\tau|\mathbf{e}_i)$, for the individual LHS elements $\mathbf{e}_i$, $i=1, 2,\ldots,300$, are shown in Fig. 9a and c. The

Please cite this article as: Helton JC, et al. Uncertainty and sensitivity analysis in performance assessment for the proposed high-level radioactive waste repository at Yucca Mountain, Nevada. Reliab Eng Syst Safety (2011), doi:10.1016/j.ress.2011.07.002

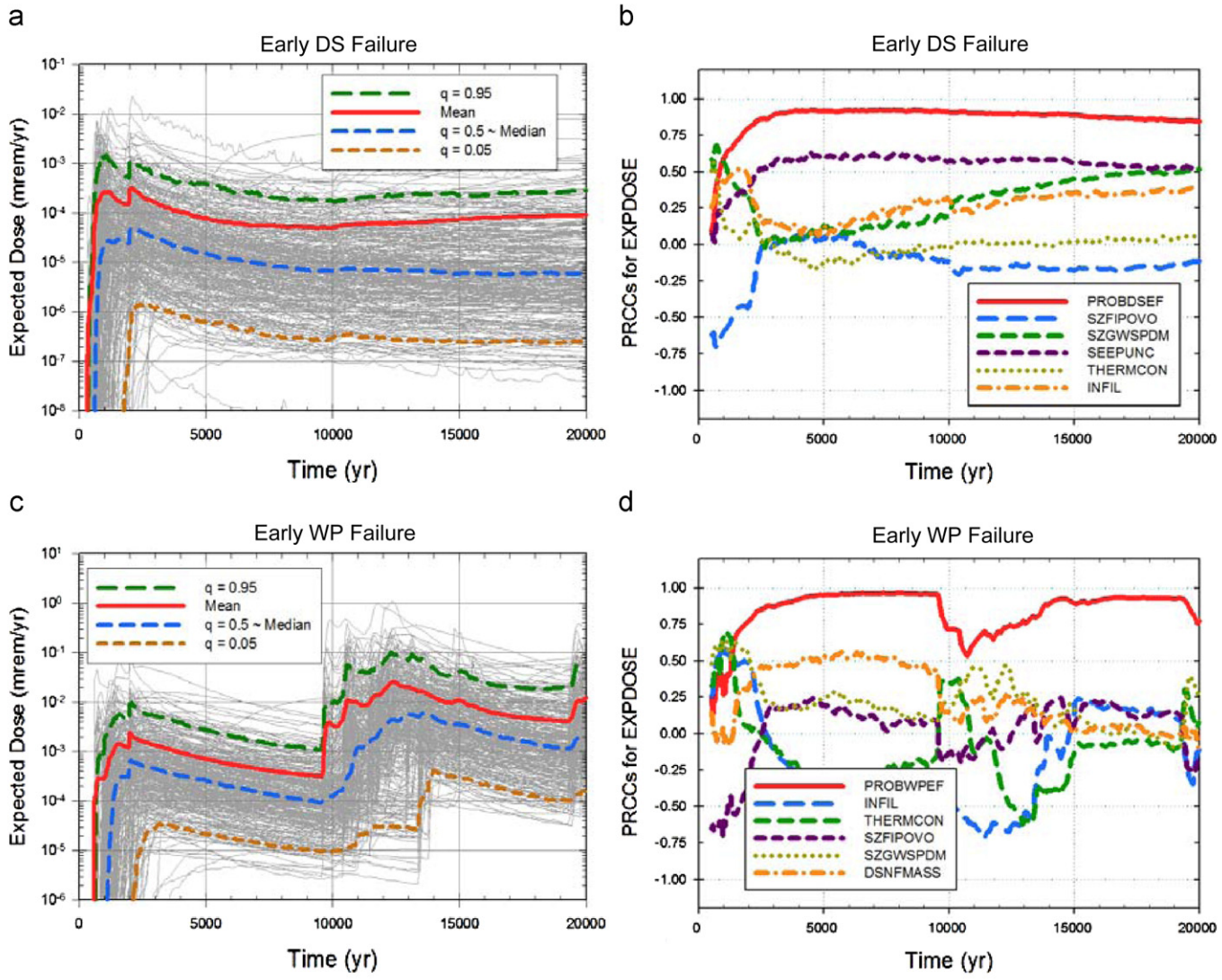

Fig. 8. Expected dose (*EXPDOSE*) to RMEI (mrem/yr) over $[0, 2 \times 10^4$ yr] for all radioactive species resulting from early failures: (a, b) $\overline{D}_{ED}(\tau|\mathbf{e})$ and associated PRCCs for early DS failure ([11], Fig. 1a,b and [6], Fig. K5.7.1-1[a]), and (c, d) $\overline{D}_{EW}(\tau|\mathbf{e})$ and associated PRCCs for early WP failure ([11], Fig. 1c,d and [6], Fig. K5.7.2-1[a]).

smoothness evident in these curves results from the use of quadrature procedures in the evaluation of expected dose (Table 4; [6], App. J). As shown by the spread of the individual curves, considerable uncertainty exists with respect to the values for $\overline{D}_{II}(\tau|\mathbf{e}_i)$ and $\overline{D}_{IE}(\tau|\mathbf{e}_i)$. Sensitivity analyses for $\overline{D}_{II}(\tau|\mathbf{e}_i)$ and $\overline{D}_{IE}(\tau|\mathbf{e}_i)$ based on PRRCs are presented in Fig. 9b and d (see Table 2 for definitions of individual variables). The dominant variables with respect to the uncertainty in $\overline{D}_{II}(\tau|\mathbf{e}_i)$ and $\overline{D}_{IE}(\tau|\mathbf{e}_i)$ are the occurrence rates *IGRATE* and *IGERATE*, respectively, with $\overline{D}_{II}(\tau|\mathbf{e}_i)$ and $\overline{D}_{IE}(\tau|\mathbf{e}_i)$ increasing as *IGRATE* and *IGERATE* increase.

The physical processes associated with igneous intrusive events and igneous eruptive events that result in dose to the RMEI are very different ([6], Section 6.5, [44]). After an igneous intrusion, radionuclide transport and exposure to the RMEI involve contaminated groundwater; in contrast, radionuclide transport and exposure after an igneous eruption primarily involve atmospheric and surficial processes. As a result, the variables selected after *IGRATE* and *IGERATE* in Fig. 9b and d are very different. Specifically, analysis for $\overline{D}_{II}(\tau|\mathbf{e})$ in Fig. 9b indicates effects for variables that influence the movement of water through the natural system (*SZGWSPDM*, *INFIL*, *SZFIPOVO* and *SZCOLRAL*) and the contribution of ^{99}Tc to dose to the RMEI (*MICTC99*). The analysis for $\overline{D}_{IE}(\tau|\mathbf{e})$ in Fig. 9d indicates effects for variables related to the uncertainty in dose to the RMEI by inhalation of contaminated particles (*INHLTPV*), the diffusion of radionuclides downward out of surface soils (*DDIVIDE*), the mass of radionuclides in WPs (*CSNFMASS*), and the attachment of waste particles to ash particles (*DASHAVG*).

5.3. Seismic scenario classes

Two seismic scenario classes are considered in the 2008 YM PA: the seismic ground motion scenario class $\mathcal{A}_{SG}$ and the seismic fault displacement scenario class $\mathcal{A}_{SF}$ (Table 1). The occurrence of seismic ground motion events and seismic fault displacement events are modeled as Poisson processes defined by underlying hazard curves that define the annual exceedance frequencies for seismic ground motion events and seismic fault displacement events of different sizes ([6], Section 6.6, [44]). A seismic ground motion event that damages WPs is assumed to cause the same damage to all WPs in the repository; in contrast, a seismic fault displacement event damages a relatively small number of WPs.

The time-dependent expected doses to the RMEI from seismic ground motion events, $\overline{D}_{SG}(\tau|\mathbf{e}_i)$, and from seismic fault

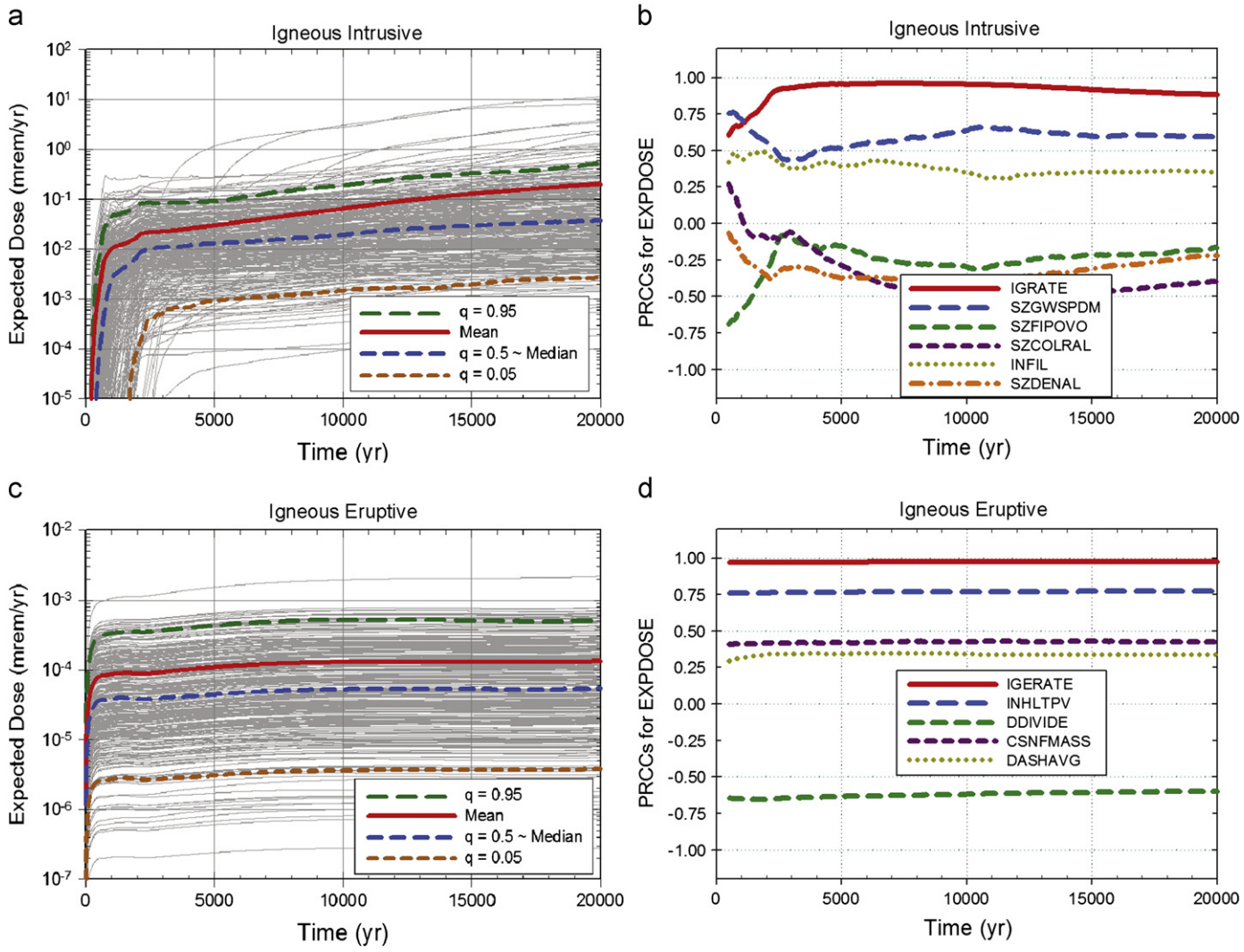

Fig. 9. Expected dose (*EXPDOSE*) to RMEI (mrem/yr) over $[0, 2 \times 10^4$ yr] for all radioactive species resulting from igneous events: (a, b) $\overline{D}_{II}(\tau|\mathbf{e})$ and associated PRCCs for igneous intrusive events ([11], Fig. 2a,b and [6], Fig. K6.7.1-1[a]), and (c, d) $\overline{D}_{IE}(\tau|\mathbf{e})$ and associated PRCCs for igneous eruptive events ([11], Fig. 2c,d and [6], Fig. K6.8.1-1).

displacement events, $\overline{D}_{SF}(\tau|\mathbf{e}_i)$, for the individual LHS elements $\mathbf{e}_i$, $i=1,2,\ldots,300$, are shown in Fig. 10a and c. The spread of the individual curves shows that considerable uncertainty exists with respect to the values for $\overline{D}_{SG}(\tau|\mathbf{e}_i)$ and $\overline{D}_{SF}(\tau|\mathbf{e}_i)$. Sensitivity analyses for $\overline{D}_{SG}(\tau|\mathbf{e})$ and $\overline{D}_{SF}(\tau|\mathbf{e})$ based on PRCCs are presented in Fig. 10b and d (see Table 2 for definitions of individual variables). The dominant variable with respect to the uncertainty in $\overline{D}_{SG}(\tau|\mathbf{e})$ is *SCCTHRP*, with $\overline{D}_{SG}(\tau|\mathbf{e})$ decreasing as *SCCTHRP* increases. The strong effect associated with *SCCTHRP* results because *SCCTHRP* defines the residual stress level at which WPs are considered to be damaged by seismically induced impacts. The 2008 YM PA uses a mean hazard curve to define the annual exceedance frequencies for seismic ground motion events of different magnitudes; as a result, no variable related to the occurrence of seismic events is present in the sensitivity analysis. After *SCCTHRP*, the analyses for $\overline{D}_{SG}(\tau|\mathbf{e})$ indicate effects for variables that influence movement of water through the natural system (*SZFIPOVO*, *SZGWSPDM* and *INFIL*), the mass of radionuclides in the disposed waste (*DSNFMASS*), and the contribution of ^{99}Tc to dose to the RMEI (*MICTC99*). An analysis of the effects of hazard curve uncertainty is presented in Ref. [122].

For $\overline{D}_{SF}(\tau|\mathbf{e})$, effects are indicated for variables related to the movement of water through the engineered and natural barriers (*SZGWSPDM*, *INFIL*, *SEEPUNC*, *SZFIPOVO* and *SEEPPRM*) and the contribution of ^{99}Tc to dose to the RMEI (*MICTC99*). However, unlike the analysis for $\overline{D}_{SG}(\tau|\mathbf{e})$, no single variable dominates the uncertainty in $\overline{D}_{SF}(\tau|\mathbf{e})$.

5.4. All failure scenario classes

Expected dose results for individual scenario classes are presented in Sections 5.1–5.3. As discussed in Sections 2.3 and 2.4, the expected dose $\overline{D}(\tau|\mathbf{e})$ for all scenario classes results from adding the incremental expected doses for the individual scenario classes. Specifically, the expected doses $\overline{D}(\tau|\mathbf{e}_i)$ in Fig. 11a for the time period $[0, 2 \times 10^4$ yr] result from adding the expected doses in Figs. 8–10 for corresponding LHS elements $\mathbf{e}_i$, $i=1,2,\ldots,300$. Similarly, the total expected doses $\overline{D}(\tau|\mathbf{e}_i)$ in Fig. 11c for the time period $[0,10^6$ yr] result from adding the expected doses for the individual scenario classes for this time period. Additional detail is provided in an extensive analysis report ([6], App. J).

In turn, the total expected doses $\overline{D}(\tau|\mathbf{e}_i)$ in Fig. 11a and c can be used to estimate mean doses $\overline{\overline{D}}(\tau)$ over aleatory and epistemic uncertainty and quantiles $Q_{Eq}[\overline{D}(\tau|\mathbf{e})]$ (e.g., $q=0.05$, 0.5, 0.95) for $\overline{D}(\tau|\mathbf{e})$ that derive from epistemic uncertainty. Values for $\overline{\overline{D}}(\tau)$ and $Q_{Eq}[\overline{D}(\tau|\mathbf{e})]$, $q=0.05$, 0.5, 0.95, are shown in Fig. 11a and c. The 2008 YM PA uses the mean dose $\overline{\overline{D}}(\tau)$ in comparisons with the 15 and 100 mrem/yr dose standards specified by the NRC for the

Please cite this article as: Helton JC, et al. Uncertainty and sensitivity analysis in performance assessment for the proposed high-level radioactive waste repository at Yucca Mountain, Nevada. Reliab Eng Syst Safety (2011), doi:10.1016/j.ress.2011.07.002

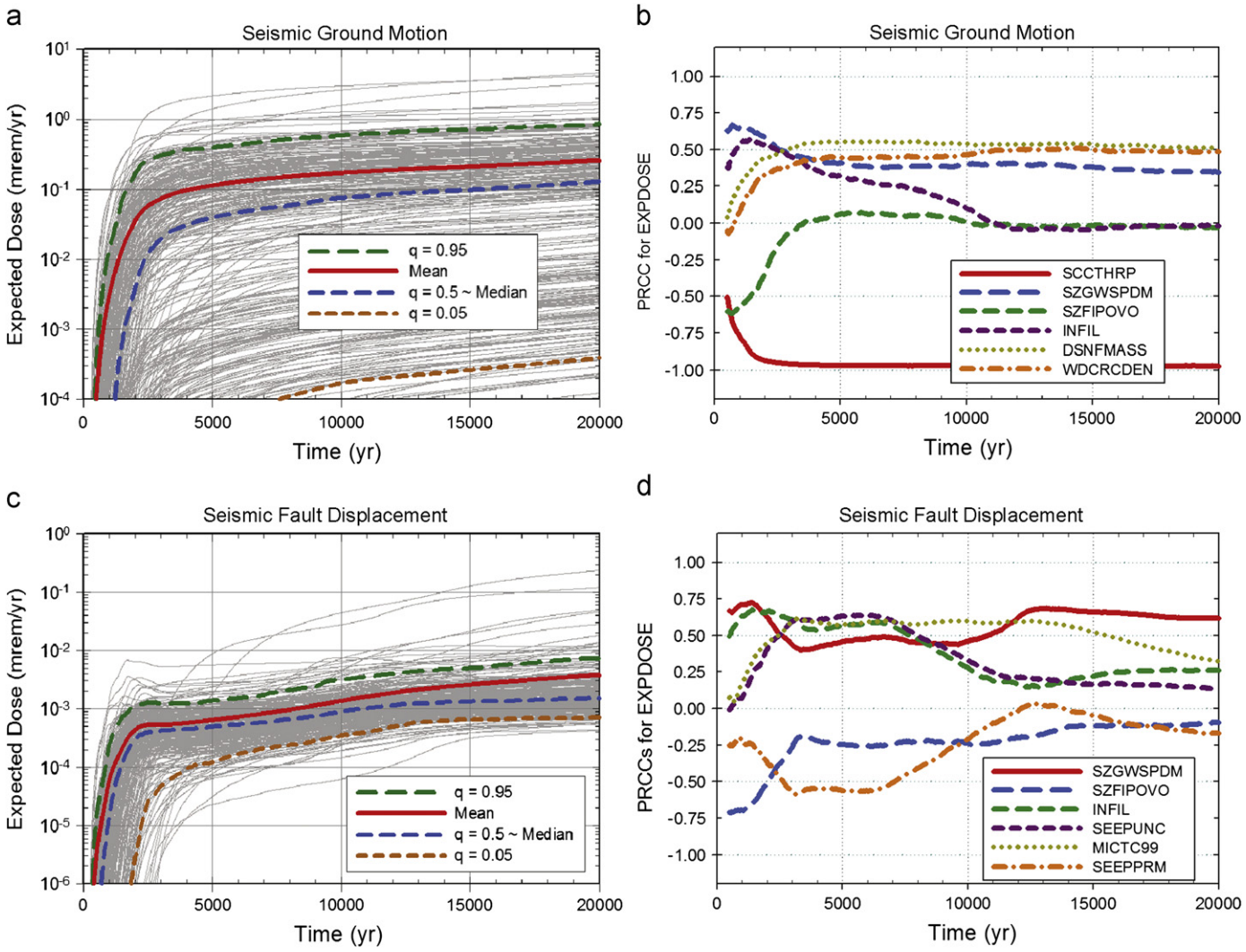

Fig. 10. Expected dose (*EXPDOSE*) to RMEI (mrem/yr) over $[0,2 \times 10^4$ yr]for all radioactive species resulting from seismic events: (a, b) $\overline{D}_{SG}(\tau|\mathbf{e})$ and associated PRCCs for seismic ground motion events ([11], Fig. 3a,b and [6], Fig. K7.7.1.-1[a]), and (c, d) $\overline{D}_{SF}(\tau|\mathbf{e})$ and associated PRCCs for seismic fault displacement events ([11], Fig. 3c,d and [6], Fig. K7.8.1.-1[a]).

time periods [0, 10^4 yr] and [10^4, 10^6 yr], respectively. If the proposed standard in (NRC1) and (NRC2) had become final, then the median expected dose $Q_{E,0.5}[\overline{D}(\tau|\mathbf{e})]$ would have been used in comparisons with the 350 mrem/yr dose standard for the [10^4, 10^6 yr] time period.

The expected dose $\overline{D}(\tau|\mathbf{e})$ for the time period $[0, 2 \times 10^4$ yr] is primarily determined by the expected dose from seismic ground motion with a secondary contribution from the expected dose from igneous intrusion ([6], Fig. 8.1-3[a]). All other scenario classes have a marginal contribution to $\overline{D}(\tau|\mathbf{e})$. For the time period [0,10^6 yr], $\overline{D}(\tau|\mathbf{e})$ is also primarily determined by the seismic ground motion and igneous intrusive scenario classes.

The smoothness evident in the expected dose results for the time period $[0, 2 \times 10^4$ yr] results from the quadrature procedure used to evaluate the expected dose from seismic ground motion for this time period (Table 4; [6], App. J). In contrast, the Monte Carlo procedure used to evaluate expected dose from the combination of seismic ground motion and nominal corrosion processes for the time period [0, 10^6 yr] results in the spikes in the curves for total expected dose evident in Fig. 11c for individual sample elements. The small jumps in total expected (mean) dose and quantiles for total expected dose appearing at 300K yr, 500K yr and 700K yr result from time steps in the thermal process model ([6], Section 8.2.4[a]). Although these spikes could be smoothed by use of a larger sample size and more refined time steps in the estimation of $\overline{D}(\tau|\mathbf{e})$, the sample sizes employed are sufficient to yield a stable estimate of the mean dose and median expected dose [123].

As shown by the spread of the results in Fig. 11a and c, a substantial amount of uncertainty is present in the estimation of $\overline{D}(\tau|\mathbf{e})$. The sensitivity analyses in Fig. 11b and d indicate the variables that are giving rise to the uncertainty in $\overline{D}(\tau|\mathbf{e})$. The PRCCs in Fig. 11b indicate that the uncertainty in $\overline{D}(\tau|\mathbf{e})$ for the time interval $[0, 2 \times 10^4$ yr] is dominated by *SCCTHRP* (see Table 2 for definitions of individual variables), reflecting the dominant contribution to total expected dose from the expected dose from seismic ground motion, and the importance of this variable to the expected dose from seismic ground motion. Smaller effects are evident from the frequency of igneous events (*IGRATE*), from variables that influence movement of water (*SZGWSPDM*, *SZFIPOVO* and *INFIL*), and from the contribution of ^{14}C to dose to the RMEI (*MICC14*) (the contribution of ^{99}Tc to the uncertainty in expected dose is slightly less than the contributions from the variables identified in Fig. 11b). For the time period [0,10^6 yr], the PRCCs in Fig. 11d indicate that the three most important variables with respect to the uncertainty in $\overline{D}(\tau|\mathbf{e})$ for this time interval are

Please cite this article as: Helton JC, et al. Uncertainty and sensitivity analysis in performance assessment for the proposed high-level radioactive waste repository at Yucca Mountain, Nevada. Reliab Eng Syst Safety (2011), doi:10.1016/j.ress.2011.07.002

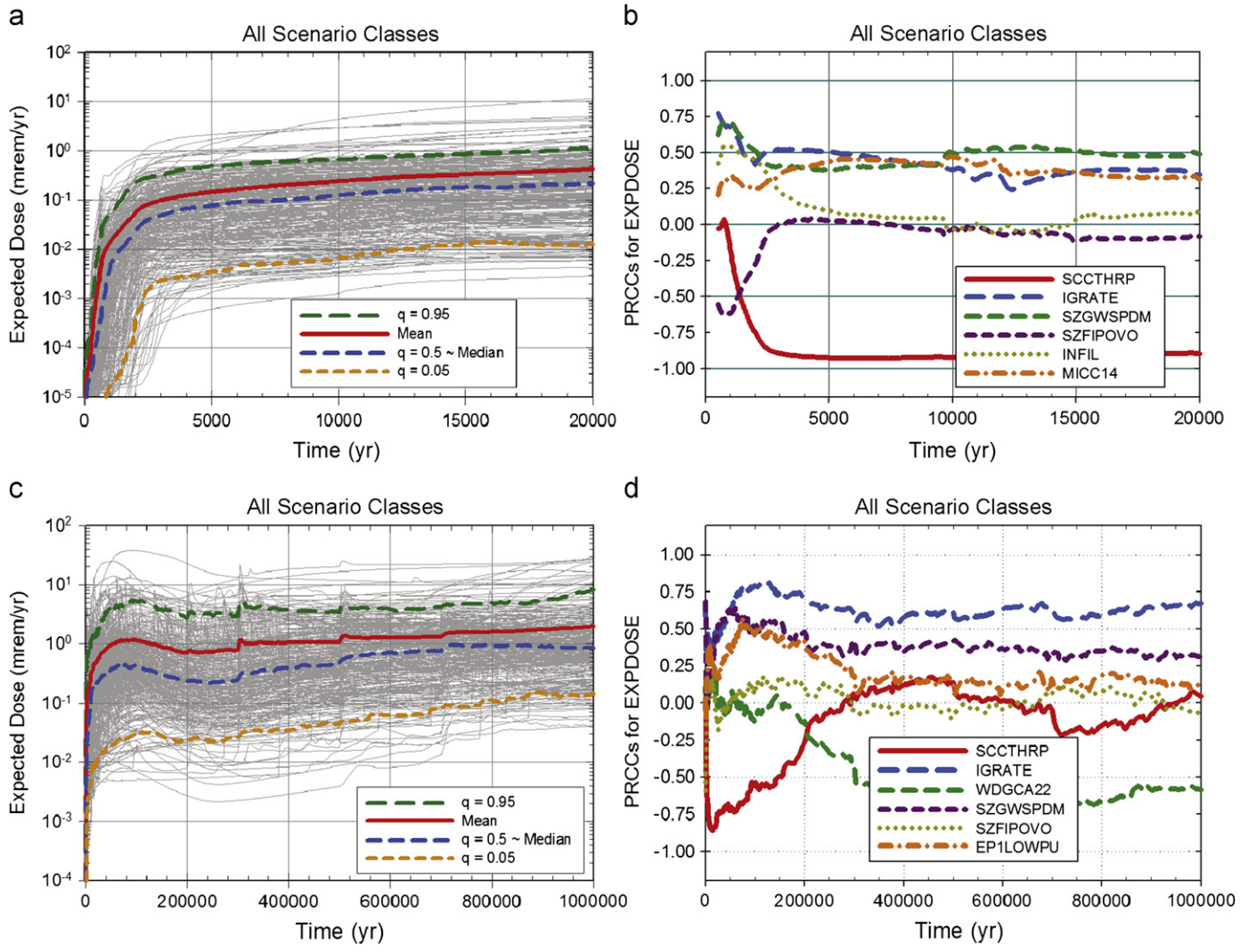

Fig. 11. Expected dose (*EXPDOSE*) to RMEI (mrem/yr) for all radioactive species and all scenario classes: (a, b) $\overline{D}(\tau|\mathbf{e})$ and associated PRCCs for $[0, 2 \times 10^4$ yr] ([11], Fig. 4a,b and [6], Fig. K8.1.-1[a]), and (c, d) $\overline{D}(\tau|\mathbf{e})$ and associated PRCCs for $[0,10^6$ yr] ([11], Fig. 4c,d and [6], Fig. K8.2.-1[a]).

SCCTHRP, *IGRATE* and *WDGCA22*. In turn, *SCCTHRP* is the dominant variable affecting the uncertainty in expected dose $\overline{D}_{SG}(\tau|\mathbf{e})$ from seismic ground motion events; *IGRATE* is the dominant variable affecting the uncertainty in expected dose $\overline{D}_{II}(\tau|\mathbf{e})$ from igneous intrusive events; and *WDGCA22* is the dominant variable affecting the uncertainty in the dose $\overline{D}_{N}(\tau|\mathbf{e})$ from nominal processes. In addition, smaller effects are indicated for *SZGWSPDM*, *SZFIPOVO*, and uncertainty in plutonium solubility (*EP1LOWPU*).

6. Summary

The importance of an appropriate assessment of the uncertainty present in PAs for the proposed YM repository for high-level radioactive waste has been strongly emphasized by the NRC (e.g., see Quotes (NRC4) and (NRC5)). In response, the 2008 YM PA was designed to maintain a separation of aleatory and epistemic uncertainty and to facilitate extensive sampling-based uncertainty and sensitivity analyses.

As described, the conceptual and computational structure of the 2008 YM PA is predicated on three basic entities: EN1, a characterization of the uncertainty in the occurrence of future events that could affect the performance of the repository (i.e., a probability space $(\mathcal{A}, \mathbb{A}, p_A)$ characterizing aleatory uncertainty); EN2, models for predicting the physical behavior and evolution of the repository system (i.e., a very complex function $D(\tau|\mathrm{a},\mathrm{e}_M)$ that predicts dose to the RMEI and a large number of additional analysis results); and EN3, a characterization of the uncertainty associated with analysis inputs that have fixed but imprecisely known values (i.e., a probability space $(\mathcal{E}, \mathbb{E}, p_E)$ characterizing epistemic uncertainty). With this design structure, it is possible to perform uncertainty and sensitivity analyses to determine the effects of epistemic uncertainty on both results conditional on specific realizations **a** of aleatory uncertainty and results that are expected values over aleatory uncertainty. In particular, expected doses over aleatory uncertainty and over both aleatory uncertainty and epistemic uncertainty are fundamental components of the NRC's regulations for the YM repository.

The 2008 YM PA used Latin hypercube sampling in the propagation of epistemic uncertainty and employed a variety of sensitivity procedures to explore the resultant mappings between uncertain analysis inputs and analysis results. Specifically, an LHS of size 300 from 392 epistemically uncertain analysis inputs was used. The primary procedures used in sensitivity analysis were examination of scatterplots, stepwise rank regression, and partial rank correlation. Further, replicated sampling was used to establish that a sample size of 300 was adequate for the propagation of epistemic uncertainty [123–125]. Although not extensively used,

Please cite this article as: Helton JC, et al. Uncertainty and sensitivity analysis in performance assessment for the proposed high-level radioactive waste repository at Yucca Mountain, Nevada. Reliab Eng Syst Safety (2011), doi:10.1016/j.ress.2011.07.002

other procedures to examine the mapping between uncertain analysis inputs and analysis results also exist, including statistical tests for patterns based on gridding ([63], Section 6.6, [69]), entropy tests for patterns based on gridding ([63], Section 6.7), nonparametric regression ([63], Section 6.8, [126–128]), squared rank differences/rank correlation test ([63], Section 6.9), two-dimensional Kolmogorov–Smirnov test ([63], Section 6.10), tests for patterns based on distance measures ([63], Section 6.11), and top down coefficient of concordance with replicated sampling ([63], Section 6.12). Complete variance decomposition procedures are also very appealing techniques for sensitivity analysis ([63], Section 6.13, [92,97,98]) but require a different sampling strategy from the one used in the 2008 YM PA and also considerably larger sample sizes.

The performance of uncertainty and sensitivity analysis in the 2008 YM PA produced a number of benefits, including: (i) permitting analysts to objectively assess the uncertainty present in the models that they developed and/or used, (ii) providing a rigorously derived assessment of the uncertainty present in analysis results, (iii) providing insights into the relationships between uncertainty in individual analysis inputs and the uncertainty in analysis results, (iv) extensively exercising the models in use and thereby contributing to analysis verification, (v) aiding decision makers by explicitly representing the uncertainty in the results that underlie their decisions, and (vi) enhancing the overall credibility of the analysis.

The appropriate disposal of radioactive waste from military and commercial activities is a challenge of national and international importance [129–144]. Uncertainty and sensitivity analysis plays an important role in the development of potential solutions for radioactive waste disposal by (i) providing guidance on how to appropriately invest analysis resources, (ii) contributing to analysis verification, and (iii) establishing that regulatory requirements can be met with a high degree of confidence. Uncertainty and sensitivity analysis played a similar role in the successful development and licensing of the Waste Isolation Pilot Plant for the geologic disposal of transuranic radioactive waste [118,121].

Acknowledgments

Work performed at Sandia National Laboratories (SNL), which is a multiprogram laboratory operated by Sandia Corporation, a Lockheed Martin Company, for the U.S. Department of Energy's (DOE's) National Nuclear Security Administration under Contract no. DE-AC04-94AL85000. The United States Government retains and the publisher, by accepting this article for publication, acknowledges that the United States Government retains a non-exclusive, paid-up, irrevocable, world-wide license to publish or reproduce the published form of this article, or allow others to do so, for United States Government purposes. The views expressed in this article are those of the authors and do not necessarily reflect the views or policies of the DOE or SNL.

References

[1] U.S. DOE (U.S. Department of Energy). Final environmental impact statement for a geologic repository for the disposal of spent nuclear fuel and high-level radioactive waste at Yucca Mountain. Nye County, Nevada.DOE/EIS-0250F.Washington, D.C.: U.S. Department of Energy Office of Civilian Radioactive Waste Management; 2002.

[2] U.S. DOE (U.S. Department of Energy). Yucca Mountain science and engineering report, Rev. 1.DOE/RW-05391. Washington, D.C.: U.S. Department of Energy Office of Civilian Radioactive Waste Management; 2002.

[3] CRWMS M&O (Civilian Radioactive Waste Management System Management and Operating Contractor). Total system performance assessment for the site recommendation.TDR-WIS-PA-000001 REV 00. Las Vegas, NV: CRWMS M&O; 2000.

[4] U.S. DOE (U.S. Department of Energy). Viability assessment of a repository at Yucca Mountain. DOE/RW-0508. Washington, D.C.: U.S. Department of Energy Office of Civilian Radioactive Waste Management; 1998.

[5] USGS (U.S. Geological Survey). Yucca Mountain as a radioactive waste repository. Circular 1184. Denver, CO: USGS Information Services 1999.

[6] SNL (Sandia National Laboratories). Total system performance assessment model/analysis for the license application. MDL-WIS-PA-000005 Rev 00, AD 01. Las Vegas, NV: U.S. Department of Energy Office of Civilian Radioactive Waste Management; 2008.

[7] U.S. DOE (U. S. Department of Energy). Yucca Mountain repository license application. DOE/RW-0573, Rev. 0. Las Vegas, NV: U. S. Department of Energy; 2008.

[8] Helton JC, Hansen CW, Sallaberry CJ. Uncertainty and sensitivity analysis in performance assessment for the proposed repository for high-level radioactive waste at Yucca Mountain, Nevada. Procedia—Social and Behavioral Sciences 2010;2:7580–2.

[9] Helton JC, Hansen CW, Sallaberry CJ. Yucca Mountain 2008 performance assessment: conceptual structure and computational implementation. In: Proceedings of the international high-level radioactive waste management conference, American Nuclear Society, September 7–11, 2008. p. 524–32.

[10] Sallaberry CJ, Aragon A, Bier A, Chen Y, Groves JW, Hansen CW, et al. Yucca Mountain 2008 performance assessment: uncertainty and sensitivity analysis for physical processes. In: Proceedings of the 2008 international high-level radioactive waste management conference, American Nuclear Society, September 7–11, 2008. p. 559–66.

[11] Hansen CW, Brooks K, Groves JW, Helton JC, Lee PL, Sallaberry CJ, et al. Yucca Mountain 2008 performance assessment: uncertainty and sensitivity analysis for expected dose. In: Proceedings of the 2008 international high-level radioactive waste management conference, September 7–11, American Nuclear Society, 2008. p. 567–74.

[12] Helton JC, Hansen CW, Sallaberry CJ. Conceptual structure of performance assessments for the geologic disposal of radioactive waste. In: 10th international probabilistic safety assessment & management conference. Seatle, WA, 2010.

[13] Hansen CW, Helton JC, Sallaberry CJ. Characterization, propagation and analysis of aleatory and epistemic uncertainty in the 2008 performance assessment for the proposed repository for high-level radioactive waste at Yucca Mountain, Nevada. Lecture Notes in Computer Science (including subseries Lecture Notes in Artificial Intelligence and Lecture Notes in Bioinformatics) 2010. 6379 LNAI: 177–190.

[14] Helton JC, Hansen CW, Sallaberry CJ. Model uncertainty in performance assessment for the proposed Yucca Mountain repository for high-level radioactive waste. In: Mosleh A, editor. Model uncertainty: conceptual and practical issues in risk-informed decision making context; 2011.

[15] Helton JC, Sallaberry CJ. Treatment of uncertainty in performance assessments for the geological disposal of radioactive waste. In: Ahn J, Apted MJ, editors. Geological repositories for safe disposal of spent fuels and radioactive materials: advanced technologies. Cambridge, UK: Woodhead Publishing; 2010. p. 547–79.

[16] Public Law 102-486. Energy Policy Act of 1992, 1992.

[17] U.S. EPA (U.S. Environmental Protection Agency). 40 CFR Part 197: public health and environmental protection standards for Yucca Mountain, NV; final rule. Federal Register 2001;66(114):32074–135.

[18] U.S. NRC (U.S. Nuclear Regulatory Commission). 10 CFR Parts 2, 19, 20, etc.: Disposal of high-level radioactive wastes in a proposed geologic repository at Yucca Mountain, Nevada; final rule. Federal Register 2001;66(213):55732–816.

[19] U.S. NRC (U.S. Nuclear Regulatory Commission). Yucca Mountain Review Plan, Final Report. NUREG-1804, Rev. 2.Washington, D.C.: U.S. Nuclear Regulatory Commission 2003.

[20] Nuclear Energy Institute v. Environmental Protection Agency. 373 F.3d 1 (D.C. Cir. 2004) (NEI) (Docket no. OAR-2005-0083-0080).

[21] NAS/NRC (National Academy of Sciences/National Research Council). Technical bases for Yucca Mountain standards. Washington, DC: National Academy Press; 1995.

[22] U.S. EPA (U.S. Environmental Protection Agency). 40 CFR Part 197: public health and environmental radiation protection standards for Yucca Mountain, Nevada; proposed rule. Federal Register 2005;10(161):49014–65.

[23] U.S. NRC (U.S. Nuclear Regulatory Commission). 10 CFR Part 63: implementation of a dose standard after 10,000 years. Federal Register 2005;70(173):53313–20.

[24] Kaplan S, Garrick BJ. On the quantitative definition of risk. Risk Analysis 1981;1(1):11–27.

[25] U.S. NRC (U.S. Nuclear Regulatory Commission). 10 CFR part 63: implementation of a dose standard after 10,000 years. Federal Register 2009;74(48):10811–30.

[26] U.S. EPA (United States Environmental Protection Agency). 40 CFR Part 197: public health and environmental radiation protection standards for Yucca Mountain. Federal Register 2008;73:61256–89.

[27] Helton JC, Sallaberry CJ. Conceptual basis for the definition and calculation of expected dose in performance assessments for the proposed high-level radioactive waste repository at Yucca Mountain, Nevada. Reliability Engineering and System Safety 2009;94:677–98.

[28] Helton JC, Sallaberry CJ. Computational implementation of sampling-based approaches to the calculation of expected dose in performance assessments for the proposed high-level radioactive waste repository at Yucca Mountain, Nevada. Reliability Engineering and System Safety 2009;94:699–721.

Please cite this article as: Helton JC, et al. Uncertainty and sensitivity analysis in performance assessment for the proposed high-level radioactive waste repository at Yucca Mountain, Nevada. Reliab Eng Syst Safety (2011), doi:10.1016/j.ress.2011.07.002

[29] Helton JC. Mathematical and numerical approaches in performance assessment for radioactive waste disposal: dealing with uncertainty. In: Scott EM, editor. Modelling radioactivity in the environment. New York, NY: Elsevier Science; 2003. p. 353–90.

[30] Helton JC, Anderson DR, Jow H-N, Marietta MG, Basabilvazo G. Conceptual structure of the 1996 performance assessment for the waste isolation pilot plant. Reliability Engineering and System Safety 2000;69(1–3):151–65.

[31] Helton JC. Uncertainty and sensitivity analysis in the presence of stochastic and subjective uncertainty. Journal of Statistical Computation and Simulation 1997;57(1–4):3–76.

[32] Helton JC, Burmaster DE. Guest editorial: treatment of aleatory and epistemic uncertainty in performance assessments for complex systems. Reliability Engineering and System Safety 1996;54(2–3):91–4.

[33] Paté-Cornell ME. Uncertainties in risk analysis: six levels of treatment. Reliability Engineering and System Safety 1996;54(2–3):95–111.

[34] Winkler RL. Uncertainty in probabilistic risk assessment. Reliability Engineering and System Safety 1996;54(2–3):127–32.

[35] Hoffman FO, Hammonds JS. Propagation of uncertainty in risk assessments: the need to distinguish between uncertainty due to lack of knowledge and uncertainty due to variability. Risk Analysis 1994;14(5):707–12.

[36] Helton JC. Treatment of uncertainty in performance assessments for complex systems. Risk Analysis 1994;14(4):483–511.

[37] Apostolakis G. The concept of probability in safety assessments of technological systems. Science 1990;250(4986):1359–64.

[38] Haan CT. Parametric uncertainty in hydrologic modeling. Transactions of the ASAE 1989;32(1):137–46.

[39] Parry GW, Winter PW. Characterization and evaluation of uncertainty in probabilistic risk analysis. Nuclear Safety 1981;22(1):28–42.

[40] Parry GW. The characterization of uncertainty in probabilistic risk assessments of complex systems. Reliability Engineering and System Safety 1996;54(2–3):119–26.

[41] Feller W. 2nd ed.An introduction to probability theory and its applications, vol. 2. New York, NY: John Wiley & Sons; 1971.

[42] Mackinnon RJ, Behie A, Chipman V, Chen Y, Lee J, Lee PL, et al.. Yucca Mountain 2008 performance assessment: modeling the engineered barrier system. In: Proceedings of the 2008 international high-level radioactive waste management conference, American Nuclear Society, September 7–11, 2008. p. 542–8.

[43] Mattie PD, Hadgu T, Lester B, Smith A, Wasiolek M, Zwahlen E. Yucca Mountain 2008 performance assessment: modeling the natural system. In. Proceedings of the 2008 international high-level radioactive waste management conference, American Nuclear Society, September 7–11, 2008. p. 550–8.

[44] Sevougian SD, Behie A, Bullard B, Chipman V, Gross MB, Stathum W. Yucca Mountain 2008 performance assessment: modeling disruptive events and early failures. In. Proceedings of the 2008 international high-level radioactive waste management conference, American Nuclear Society, September 7–11, 2008. p. 533–41.

[45] SNL (Sandia National Laboratories). Atmospheric dispersal and deposition of tephra from a potential volcanic eruption at Yucca Mountain, Nevada. MDL-MGR-GS-000002 REV 03. Las Vegas, NV: U.S. Department of Energy Office of Civilian Radioactive Waste Management; 2007.

[46] SNL (Sandia National Laboratories). Engineered barrier system: physical and chemical environment. ANL-EBS-MD-000033 REV 06. Las Vegas, NV: Sandia National Laboratories; 2007.

[47] SNL (Sandia National Laboratories). Initial radionuclide inventories. ANL-WIS-MD-000020 REV 01 ADD 01. Las Vegas, NV: U.S. Department of Energy Office of Civilian Radioactive Waste Management; 2007.

[48] SNL (Sandia National Laboratories). Dissolved concentration limits of elements with radioactive isotopes. ANL-WIS-MD-000010 REV 06. Las Vegas, NV: U.S. Department of Energy Office of Civilian Radioactive Waste Management; 2007.

[49] SNL (Sandia National Laboratories). Number of waste packages hit by igneous events. ANL-MGR-GS-000003 REV 03. Las Vegas, NV: U.S. Department of Energy Office of Civilian Radioactive Waste Management; 2007.

[50] BSC (Bechtel SAIC Company). Characterize framework for igneous activity at Yucca Mountain, Nevada. ANL-MGR-GS-000001 REV 02. Las Vegas, NV: Bechtel SAIC Company; 2004.

[51] SNL (Sandia National Laboratories). Biosphere model report. MDL-MGR-MD-000001 REV 02. Las Vegas, Nevada: U.S. Department of Energy Office of Civilian Radioactive Waste Management; 2007.

[52] SNL (Sandia National Laboratories). Analysis of mechanisms for early waste package/drip shield failure. ANL-EBS-MD-000076 REV 00. Las Vegas, NV: U.S. Department of Energy Office of Civilian Radioactive Waste Management; 2007.

[53] SNL (Sandia National Laboratories). Stress corrosion cracking of waste package outer barrier and drip shield materials. ANL-EBS-MD-000005 REV 04. Las Vegas, NV: U.S. Department of Energy Office of Civilian Radioactive Waste Management; 2007.

[54] SNL (Sandia National Laboratories). Abstraction of drift seepage. MDL-NBS-HS-000019 REV 01 ADD 01. Las Vegas, Nevada: U.S. Department of Energy Office of Civilian Radioactive Waste Management; 2007.

[55] SNL (Sandia National Laboratories). Saturated zone flow and transport model abstraction.MDL-NBS-HS-000021 REV 03 AD 02. Las Vegas, NV: U.S. Department of Energy Office of Civilian Radioactive Waste Management; 2008.

[56] SNL (Sandia National Laboratories). Multiscale thermohydrologic model. ANL-EBS-MD-000049 REV 03 ADD 01. Las Vegas, Nevada: U.S. Department of Energy Office of Civilian Radioactive Waste Management; 2007.

[57] SNL (Sandia National Laboratories). General corrosion and localized corrosion of waste package outer barrier. ANL-EBS-MD-000003 REV 03. Las Vegas, NV: U.S. Department of Energy Office of Civilian Radioactive Waste Management; 2007.

[58] McKay MD, Beckman RJ, Conover WJ. A comparison of three methods for selecting values of input variables in the analysis of output from a computer code. Technometrics 1979;21(2):239–45.

[59] Helton JC, Davis FJ. Latin hypercube sampling and the propagation of uncertainty in analyses of complex systems. Reliability Engineering and System Safety 2003;81(1):23–69.

[60] Helton JC, Iuzzolino HJ. Construction of complementary cumulative distribution functions for comparison with the EPA release limits for radioactive waste disposal. Reliability Engineering and System Safety 1993;40(3):277–93.

[61] Helton JC, Davis FJ. Sampling-based methods. In: Saltelli A, Chan K, Scott EM, editors. Sensitivity analysis. New York, NY: Wiley; 2000. p. 101–53.

[62] Iman RL, Conover WJ. The use of the rank transform in regression. Technometrics 1979;21(4):499–509.

[63] Helton JC, Johnson JD, Sallaberry CJ, Storlie CB. Survey of sampling-based methods for uncertainty and sensitivity analysis. Reliability Engineering and System Safety 2006;91(10–11):1175–209.

[64] Iman RL, Conover WJ. Small sample sensitivity analysis techniques for computer models, with an application to risk assessment. Communications in Statistics: Theory and Methods 1980;A9(17):1749–842.

[65] Iman RL, Helton JC, Campbell JE. An approach to sensitivity analysis of computer models, Part 1. Introduction, input variable selection and preliminary variable assessment. Journal of Quality Technology 1981;13(3):174–83.

[66] Iman RL, Helton JC, Campbell JE. An approach to sensitivity analysis of computer models, Part 2. Ranking of input variables, response surface validation, distribution effect and technique synopsis. Journal of Quality Technology 1981;13(4):232–40.

[67] Iman RL. Uncertainty and sensitivity analysis for computer modeling applications. In: TA Cruse (Ed.), Reliability technology—1992, The winter annual meeting of the American society of mechanical engineers, Anaheim, California, November 8–13, 1992. New York, NY: American Society of Mechanical Engineers, Aerospace Division, 1992. p. 153–68.

[68] Helton JC. Uncertainty and sensitivity analysis techniques for use in performance assessment for radioactive waste disposal. Reliability Engineering and System Safety 1993;42(2–3):327–67.

[69] Kleijnen JPC, Helton JC. Statistical analyses of scatterplots to identify important factors in large-scale simulations, 1: Review and comparison of techniques. Reliability Engineering and System Safety 1999;65(2):147–85.

[70] Helton JC, Davis FJ. Illustration of sampling-based methods for uncertainty and sensitivity analysis. Risk Analysis 2002;22(3):591–622.

[71] Cacuci DG, Schlesinger ME. On the application of the adjoint method of sensitivity analysis to problems in the atmospheric sciences. Atmósfera 1994;7(1):47–59.

[72] Cacuci DG. Sensitivity theory for nonlinear systems. I. Nonlinear functional analysis approach. Journal of Mathematical Physics 1981;22(12):2794–802.

[73] Cacuci DG. Sensitivity theory for nonlinear systems. II. Extensions to additional classes of responses. Journal of Mathematical Physics 1981;22(12):2803–12.

[74] Cacuci DG, Weber CF, Oblow EM, Marable JH. Sensitivity theory for general systems of nonlinear equations. Nuclear Science and Engineering 1980;75(1):88–110.

[75] Cacuci DG. Sensitivity and uncertainty analysis, vol. 1: theory. Boca Raton, FL: Chapman and Hall/CRC Press; 2003.

[76] Turányi T. Sensitivity analysis of complex kinetic systems. Tools and applications. Journal of Mathematical Chemistry 1990;5(3):203–48.

[77] Rabitz H, Kramer M, Dacol D. Sensitivity analysis in chemical kinetics. Annual Review of Physical Chemistry 1983;34:419–61.

[78] Lewins J, Becker M, editors. Sensitivity and uncertainty analysis of reactor performance parameters, vol. 14. New York, NY: Plenum Press; 1982.

[79] Frank PM. Introduction to system sensitivity theory. New York, NY: Academic Press; 1978.

[80] Tomovic R, Vukobratovic M. General sensitivity theory. New York, NY: Elsevier; 1972.

[81] Myers RH. Response surface methodology—current status and future directions. Journal of Quality Technology 1999;31(1):30–44.

[82] Andres TH. Sampling methods and sensitivity analysis for large parameter sets. Journal of Statistical Computation and Simulation 1997;57(1–4):77–110.

[83] Kleijnen JPC. Sensitivity analysis and related analyses: a review of some statistical techniques. Journal of Statistical Computation and Simulation 1997;57(1–4):111–42.

[84] Kleijnen JPC. Sensitivity analysis of simulation experiments: regression analysis and statistical design. Mathematics and Computers in Simulation 1992;34(3–4):297–315.

[85] Morton RH. Response surface methodology. Mathematical Scientist 1983;8:31–52.

[86] Mead R, Pike DJ. A Review of response surface methodology from a biometric viewpoint. Biometrics 1975;31:803–51.

Please cite this article as: Helton JC, et al. Uncertainty and sensitivity analysis in performance assessment for the proposed high-level radioactive waste repository at Yucca Mountain, Nevada. Reliab Eng Syst Safety (2011), doi:10.1016/j.ress.2011.07.002

[87] Myers RH. Response surface methodology. Boston, MA: Allyn and Bacon; 1971.
[88] Borgonovo E, Castaings W, Tarantola S. Moment independent importance measures: new results and analytical test cases. Risk Analysis 2011;31(3): 404–28.
[89] Borgonovo E, Tarantola S. Moment independent and variance-based sensitivity analysis with correlations: an application to the stability of a chemical reactor. International Journal of Chemical Kinetics 2008;40(11):687–98.
[90] Borgonovo EA. New uncertainty importance measure. Reliability Engineering and System Safety 2007;92(6):771–84.
[91] Borgonovo E. Measuring uncertainty importance: investigation and comparison of alternative approaches. Risk Analysis 2006;26(5):1349–61.
[92] Saltelli A, Annoni P, Azzini I, Campolongo F, Ratto M, Tarantola S. Variance based sensitivity analysis of model output. Design and estimator for the total sensitivity index. Computer Physics Communications 2010;181(2):259–70.
[93] Saltelli A, Ratto M, Andres T, Campolongo F, Cariboni J, Gatelli D, et al. Global sensitivity analysis: the primer. New York, NY: Wiley; 2008.
[94] Chan K, Tarantola S, Saltelli A. Variance-based methods. In: Saltelli A, Chan K, Scott EM, editors. Sensitivity analysis. New York, NY: Wiley; 2000. p. 167–97.
[95] Li G, Rosenthal C, Rabitz H. High-dimensional model representations. The Journal of Physical Chemistry 2001;105(33):7765–77.
[96] Rabitz H, Alis OF. General foundations of high-dimensional model representations. Journal of Mathematical Chemistry 1999;25(2–3):197–233.
[97] Saltelli A, Tarantola S, Chan KP-S. A quantitative model-independent method for global sensitivity analysis of model output. Technometrics 1999;41(1):39–56.
[98] Sobol' IM. Sensitivity estimates for nonlinear mathematical models. Mathematical Modeling & Computational Experiment 1993;1(4):407–14.
[99] Cukier RI, Levine HB, Shuler KE. Nonlinear sensitivity analysis of multiparameter model systems. Journal of Computational Physics 1978;26(1): 1–42.
[100] Iman RL, Helton JC. An investigation of uncertainty and sensitivity analysis techniques for computer models. Risk Analysis 1988;8(1):71–90.
[101] Ronen Y. Uncertainty analysis. Boca Raton, FL: CRC Press, Inc.; 1988.
[102] Hamby DM. A review of techniques for parameter sensitivity analysis of environmental models. Environmental Monitoring and Assessment 1994;32(2): 135–54.
[103] Saltelli A, Chan K, Scott EM, editors. Sensitivity analysis. New York, NY: Wiley; 2000.
[104] Frey HC, Patil SR. Identification and review of sensitivity analysis methods. Risk Analysis 2002;22(3):553–78.
[105] Ionescu-Bujor M, Cacuci DG. A Comparative review of sensitivity and uncertainty analysis of large-scale systems—I: deterministic methods. Nuclear Science and Engineering 2004;147(3):189–2003.
[106] Cacuci DG, Ionescu-Bujor M. A Comparative review of sensitivity and uncertainty analysis of large-scale systems—II: statistical methods. Nuclear Science and Engineering 2004;147(3):204–17.
[107] Saltelli A, Ratto M, Tarantola S, Campolongo F. Sensitivity analysis for chemical models. Chemical Reviews 2005;105(7):2811–28.
[108] Hall JW, Boyce SA, Wang Y, Dawson RJ, Tarantola S, Saltelli A. Sensitivity analysis for hydraulic models. Journal of Hydraulic Engineering 2009;135(11): 959–69.
[109] Marino S, Hogue IB, Ray CJ, Kirschner DE. A methodology for performing global uncertainty and sensitivity analysis in systems biology. Journal of Theoretical Biology 2008;254(1):178–96.
[110] de Rocquigny E, Devictor N, Tarantola S. Uncertainty in industrial practice: a guide to quantitative uncertainty management. Chichester, England: Wiley; 2008.
[111] U.S. NRC (U.S. Nuclear Regulatory Commission). Severe accident risks: an assessment for five U.S. nuclear power plants. NUREG-1150, vols. 1–3. Washington, DC: U.S. Nuclear Regulatory Commission, Office of Nuclear Regulatory Research, Division of Systems Research; 1990–1991.
[112] Breeding RJ, Helton JC, Gorham ED, Harper FT. Summary description of the methods used in the probabilistic risk assessments for NUREG-1150. Nuclear Engineering and Design 1992;135(1):1–27.
[113] Breeding RJ, Helton JC, Murfin WB, Smith LN, Johnson JD, Jow H-N, et al. The NUREG-1150 probabilistic risk assessment for the Surry Nuclear Power Station. Nuclear Engineering and Design 1992;135(1):29–59.
[114] Payne Jr. AC, Breeding RJ, Helton JC, Smith LN, Johnson JD, Jow H-N, et al. The NUREG-1150 Probabilistic risk assessment for the Peach Bottom Atomic Power Station. Nuclear Engineering and Design 1992;135(1):61–94.
[115] Gregory JJ, Breeding RJ, Helton JC, Murfin WB, Higgins SJ, Shiver AW. The NUREG-1150 probabilistic risk assessment for the Sequoyah Nuclear Plant. Nuclear Engineering and Design 1992;135(1):95–115.
[116] Brown TD, Breeding RJ, Helton JC, Jow H-N, Higgins SJ, Shiver AW. The NUREG-1150 probabilistic risk assessment for the Grand Gulf Nuclear Station. Nuclear Engineering and Design 1992;135(1):117–37.
[117] Helton JC, Breeding RJ. Calculation of reactor accident safety goals. Reliability Engineering and System Safety 1993;39(2):129–58.
[118] U.S. DOE (U.S. Department of Energy). Title 40 CFR Part 191 compliance certification application for the Waste Isolation Pilot Plant. DOE/CAO-1996-2184, vols. I-XXI. Carlsbad, NM: U.S. Department of Energy, Carlsbad Area Office, Waste Isolation Pilot Plant; 1996.
[119] Helton JC. Uncertainty and sensitivity analysis in performance assessment for the Waste Isolation Pilot Plant. Computer Physics Communications 1999;117(1-2):156–80.
[120] Helton JC, Anderson DR, Jow H-N, Marietta MG, Basabilvazo G. Performance assessment in support of the 1996 compliance certification application for the waste isolation pilot plant. Risk Analysis 1999;19(5):959–86.
[121] Helton JC, Marietta MG, editors. The 1996 performance assessment for the Waste Isolation Pilot Plant. Reliability Engineering and System Safety, 69; 2000. p. 1–451. (special issue).
[122] Helton JC, Sallaberry CJ. Yucca Mountain 2008 performance assessment: incorporation of seismic hazard curve uncertainty. In: Proceedings of the 13th international high-level radioactive waste management conference (IHLRWMC), Albuquerque, NM, April 10–14, 2011. American Nuclear Society, 2011. p. 1041–8.
[123] Hansen CW, Helton JC, Sallaberry CJ. Use of replicated sampling to estimate sampling variance in uncertainty and sensitivity analysis results. Reliability Engineering and System Safety, this issue.
[124] Helton JC, Davis FJ, Johnson JD. A Comparison of uncertainty and sensitivity analysis results obtained with random and Latin hypercube sampling. Reliability Engineering and System Safety 2005;89(3):305–30.
[125] Iman RL. Statistical methods for including uncertainties associated with the geologic isolation of radioactive waste which allow for a comparison with licensing criteria. In: DC Kocher, Ed. Proceedings of the symposium on uncertainties associated with the regulation of the geologic disposal of high-level radioactive waste, Gatlinburg, TN, March 9–13, 1981: Washington, DC: U.S. Nuclear Regulatory Commission, Directorate of Technical Information and Document Control, 1982. p. 145–57.
[126] Storlie CB, Helton JC. Multiple predictor smoothing methods for sensitivity analysis: description of techniques. Reliability Engineering and System Safety 2008;93(1):28–54.
[127] Storlie CB, Helton JC. Multiple predictor smoothing methods for sensitivity analysis: example results. Reliability Engineering and System Safety 2008;93(1):55–77.
[128] Storlie CB, Swiler LP, Helton JC, Sallaberry CJ. Implementation and evaluation of nonparametric regression procedures for sensitivity analysis of computationally demanding models. Reliability Engineering and System Safety 2009;94(11):1735–63.
[129] Rosa EA, et al. Nuclear waste: knowledge waste. Science 2010;329(5993): 762–3.
[130] Garrick BJ, Stetkar JW, Bembia PJ. Quantitative risk assessment of the New York state operated West Valley radioactive disposal area. Risk Analysis 2010;30(8):1219–30.
[131] Swift PN. Safety assessment for deep geological disposal of high-level radioactive waste. In: Ahn J, Apted MJ, editors. Geological repositories for safe disposal of spent nuclear fuels and radioactive materials: advanced technologies. Cambridge, UK: Woodhead Publishing; 2010. p. 497–521.
[132] Rechard RP. Historical background on performance assessment for the Waste Isolation Pilot Plant. Reliability Engineering and System Safety 2000;69(1–3):5–46.
[133] Carter LJ, Pigford TH. The world's growing inventory of civil spent fuel. Arms Control Today 1999;29(1):8–14.
[134] Ewing RC. Less geology in the geological disposal of nuclear waste. Science 1999;286:415–6.
[135] Ewing RC, Tierney MS, Konikow LK, Rechard RP. Performance assessments for nuclear waste repositories: a dialogue on their values and limitations. Risk Analysis 1999;19(5):933–58.
[136] North DW. A perspective on nuclear waste. Risk Analysis 1999;19(4):751–8.
[137] Okrent D. On intergenerational equity and its clash with intragenerational equity and on the need for policies to guide the regulation of disposal of wastes and other activities posing very long-term risks. Risk Analysis 1999;19(5):877–901.
[138] Rechard RP. Historical relationship between performance assessment for radioactive waste disposal and other types of risk assessment. Risk Analysis 1999;19(5):763–807.
[139] Ahearne JF. Radioactive waste: the size of the problem. Physics Today 1997;50(6):24–9.
[140] Crowley KD. Nuclear waste disposal: the technical challenges. Physics Today 1997;50(6):32–9.
[141] Flynn J, Kasperson RE, Kunreuther H, Slovic P. Overcoming tunnel vision: redirecting the U.S. high-level nuclear waste program. Environment 1997;39(3):25–30. 6–11.
[142] Kastenburg WE, Gratton LJ. Hazards of managing and disposing of nuclear waste. Physics Today 1997;50(6):41–6.
[143] McCombie C. Nuclear waste management worldwide. Physics Today 1997;50(6):56–62.
[144] North DW. Unresolved problems of radioactive waste: motivation for a new paradigm. Physics Today 1997;50(6):48–54.

Please cite this article as: Helton JC, et al. Uncertainty and sensitivity analysis in performance assessment for the proposed high-level radioactive waste repository at Yucca Mountain, Nevada. Reliab Eng Syst Safety (2011), doi:10.1016/j.ress.2011.07.002